# Alpha decay of spherical nuclei

S. G. Kadmenskiĭ

*Kuĭbyshev State University, Kuĭbyshev*

V. I. Furman

*Joint Institute for Nuclear Research, Dubna*

Fiz. Élem. Chastits At. Yadra, 6, 469–514 (April–June 1975)

The non-$R$-matrix approach to $\alpha$-decay theory is used to consider the possibility of describing the absolute and relative probabilities of $\alpha$ decays of spherical nuclei in the traditional shell model. The surface $\alpha$-cluster model is introduced and used to study the contribution of the asymptotic regions to the $\alpha$-decay widths and to analyze the data on $\alpha$ decay of compound states.

PACS numbers: 21.60.C, 23.60.

## INTRODUCTION

*General Properties of $\alpha$ Radioactivity*. There are currently known[1] three fairly large regions of nuclei that exhibit spontaneous $\alpha$ radioactivity: rare earths, spherical nuclei in the neighborhood of $^{208}$Pb, and transuranium elements. As a result of the progress in the method of obtaining neutron-deficient isotopes, all three regions have been significantly extended, and a new island of radioactivity has arisen in the neighborhood of $A \approx 100$. Besides these $\alpha$ emitters, intensive study is currently being made of $\alpha$ decay from excited states of light nuclei (by means of $(p,\alpha)$, $(n,\alpha)$ and other reactions) and in the intermediate range $60 \leqslant A \leqslant 180$ by means of $(n,\alpha)$ reactions with slow neutrons. Thus, the emission of $\alpha$ particles from the ground or excited states of atomic nuclei is a global phenomenon observed in virtually the whole of the periodic system of the elements.

A characteristic feature of $\alpha$ decay is the exponential sensitivity of the half-life to the energy of the $\alpha$ particle. The half-lives $T^{\alpha}_{1/2}$ therefore range over a wide interval, $10^{-20} \leqslant T^{\alpha}_{1/2} \leqslant 10^{25}$ sec, which imposes very stringent requirements on any theory which pretends to describe the absolute probabilities of $\alpha$ decay. A large body of experimental material relating to $\alpha$ decay has now been accumulated (energies and half-lives, branching ratios for different groups of $\alpha$ particles, $(\alpha,\gamma)$ correlations and $\alpha$-particle angular distributions resulting from the decay of oriented nuclei, etc). Unfortunately, it has not yet proved possible to obtain much information about the properties and detailed structure of nuclei from these experimental data.

The reason for this is the difficulties which arise in the construction of a consistent theory of $\alpha$ decay. This is due to the physical complexity of $\alpha$ decay, which must be regarded as the decay of an isolated many-particle resonance state through the $\alpha$-particle (four-nucleon) channel. Note that, in contrast to $\beta$ and $\gamma$ decay and also the problems associated with studying the structure and properties of ground states and low-lying excited states of nuclei, which are basically determined by the three-dimensional properties of the nuclear wave functions, $\alpha$ decay is a process related to surface nuclear reactions and depends essentially on the characteristics of nuclei in the peripheral region, for which information at present is by no means complete.

Therefore, understanding of $\alpha$ decay gives additional data on the properties of nuclei in the surface region and in particular the role played by $\alpha$ clustering in this region.[2]

It is only now that the first steps are being taken toward the construction of a quantitative $\alpha$-decay theory. In this review we shall be concerned with the prospects and difficulties of investigations in this direction.

*Historical Review of Many-Particle Variants of the $\alpha$-Decay Theory*. The first many-particle approach to the description of $\alpha$ decay was developed by Thomas[3] and Mang[4] in the framework of the $R$-matrix theory of nuclear reactions.[5] In Ref. 3, $\alpha$ decay is regarded as the decay of an isolated resonance with spin $I_i$, projection $M_i$, and other quantum numbers $\sigma_i$. The partial decay width in the $\alpha$-particle channel $L\sigma_f I_f$ is given by

$$\Gamma_{L\sigma_f I_f} = 2P_L(R_0)\,\gamma^2_{L\sigma_f I_f}(R_0), \tag{1}$$

where $P_L(R_0)$ is the penetration factor[5]; $R_0$ is the channel radius; the reduced-width amplitude, $\gamma_{L\sigma_f I_f}$, is determined by the overlap integral between the wave function of the initial state, $\Psi^{I_i M_i}_{\sigma_i}$, and the wave function of the final $\alpha$-decay channel, $u^{I_i M_i}_{L\sigma_f I_f}$:

$$\gamma_{L\sigma_f I_f}(R_0) = \sqrt{\frac{\hbar^2 R_0}{2m}}\,\langle \Psi^{I_i M_i}_{\sigma_i} | u^{I_i M_i}_{L\sigma_f I_f} \rangle |_{R=R_0}, \tag{2}$$

the function $u^{I_i M_i}_{L\sigma_f I_f}$ having the form

$$u^{I_i M_i}_{L\sigma_f I_f} = \sum_{M_f} C^{I_f L I_i}_{M_f M M_i} Y_{LM}(\Omega_R)\,\psi_\alpha \Psi^{I_f M_f}_{\sigma_f}. \tag{3}$$

Here, $m$ is the reduced mass of the $\alpha$ particle; $\Psi^{I_f M_f}_{\sigma_f}$ is the wave function of the daughter nucleus. The spherical function $Y_{LM}(\Omega_R)$ is the angular part of the function of the relative motion of the center of mass of an $\alpha$ particle with orbital angular momentum $L$ and projection thereof $M$.

The internal function of the $\alpha$ particle

$$\psi_\alpha = \chi_\alpha(\xi_1, \xi_2, \xi_3)\,S_\alpha(1, 2, 3, 4) \tag{4}$$

factorizes into the spin function $S_\alpha$ and the spatial function $\chi_\alpha$, which is chosen in the form

$$\chi_\alpha(\xi_1, \xi_2, \xi_3) = \left(\frac{\beta}{\pi}\right)^{9/4} \exp\left[-\frac{\beta}{2}\sum_{i=1}^{3}\xi_i^2\right]. \tag{5}$$

Here we have used the variables

$$\left.\begin{aligned}\xi_1 &= (\mathbf{r}_1-\mathbf{r}_2)/\sqrt{2};\quad \xi_3 = (\mathbf{r}_1+\mathbf{r}_2-\mathbf{r}_3-\mathbf{r}_4)/2;\\ \xi_2 &= (\mathbf{r}_3-\mathbf{r}_4)/\sqrt{2};\quad \mathbf{R} = (\mathbf{r}_1+\mathbf{r}_2+\mathbf{r}_3+\mathbf{r}_4)/4.\end{aligned}\right\} \tag{6}$$

The total $\alpha$-decay width $\Gamma$ is given by the sum of the partial widths:

$$\Gamma = \sum_{L\sigma_f I_f} \Gamma_{L\sigma_f I_f}. \tag{7}$$

In the considered variant of the theory, $\alpha$ decay is treated as a process that occurs in two stages. In the first stage, at the point $R_0$ an $\alpha$ particle and the daughter nucleus are formed in the parent nucleus with probability proportional to $\gamma^2_{L\sigma_f I_f}(R_0)$. In the second stage, the $\alpha$ particle as a whole penetrates the potential barrier with a probability proportional to $P_L(R_0)$.

Numerous calculations of $\alpha$-decay probabilities of spherical and deformed nuclei have been made[1] in the framework of Thomas and Mang's scheme. In these calculations, the wave functions of the parent and daughter nuclei are constructed on the basis of the shell model with allowance for mixing of configurations and superfluid correlations. The calculations have shown that in some cases the relative theoretical probabilities of $\alpha$ decay can agree with the corresponding theoretical values, whereas the absolute probabilities differ strongly from the experimental and, depending on the choice of the parameter $R_0$ of the theory, may vary by four or more orders of magnitude.[6]

Further progress in the understanding of $\alpha$ decay is associated with the development of non-$R$-matrix approaches, which in principle do not contain the free parameter $R_0$. The first variant of such an approach was developed by Harada and Rauscher.[7] Using Mang's method,[4] they obtained an integral formula for the partial $\alpha$-decay width:

$$\Gamma_{L\sigma_f I_f} = 2\pi |\langle \Psi^{I_i M_i}_{\sigma_i} | V_{\alpha A-4} - V^{\text{opt}}_{\alpha}(R) | u^{I_i M_i}_{L\sigma_f I_f} \varphi_L \rangle|^2, \tag{8}$$

where $V_{\alpha A-4}$ is the total nuclear potential of the interaction between the $\alpha$ particle and the daughter nucleus. The function $\varphi_L(R)$ describes the motion of the center of mass of the $\alpha$ particle in the optical potential $V^{\text{opt}}_{\alpha}(R)$.

An attractive feature of Eq. (8) is the absence of a parameter $R_0$, in which it resembles Feshbach's expression[8] for the decay width of a resonance state. For the potential $V_{\alpha A-4}$, Harada and Rauscher[7] use a sum of the real parts of the nucleon optical potentials:

$$V_{\alpha A-4} = \sum_{i=1}^{4} V_i(\mathbf{r}_i) = \sum_{i=1}^{4} V_{0i} f(r_i), \tag{9}$$

where

$$f(r_i) = [1+\exp\{(r_i - R_A)/a\}]^{-1};\qquad R_A = r_0 A^{1/3}. \tag{10}$$

The parameters $r_0$, $a$, and $V_{0i}$ can be found from experimental data on the elastic scattering of nucleons. The optical potential $V^{\text{opt}}_{\alpha}(R)$ is chosen phenomenologically in Ref. 7 without any relation to the potential $V_{\alpha A-4}$ in (9), although, as was shown later in Ref. 9, the optical potential $V^{\text{opt}}_{\alpha}(R)$ constructed on the basis of a sum of the optical nucleon potentials satisfactorily describes the $\alpha$-particle elastic-scattering data, so that the required agreement is in principle possible. On the other hand, because the integrand of Eq. (8) contains the two oscillating functions $\langle \Psi^{I_i M_i}_{\sigma_i} | u^{I_i M_i}_{L\sigma_f I_f} \rangle$ and $\varphi_L$, which are basically inconsistent with one other, the value of $\Gamma_{L\sigma_f I_f}$ changes strongly from one nucleus to another, from one potential to another, and from one energy $Q_\alpha$ to another.

As is shown in Ref. 7, the use of different sets of potentials $V^{\text{opt}}_{\alpha}$ leads to a spread in the calculated absolute $\alpha$ widths relative to the experimental widths of from $10^{-3}$ to $6\cdot 10^{-2}$ for $^{210}$Po and from 1 to $0.7\times 10^{-3}$ for $^{212}$Po. It is characteristic that one cannot find any set of potentials $V^{\text{opt}}_{\alpha}$ that simultaneously describes even these two nuclei satisfactorily: The potentials which lead to agreement with the experimental $\alpha$ widths for $^{210}$Po are very different from those for $^{212}$Po.

The sensitivity of $\Gamma_{L\sigma_f I_f}$ to the energy $Q_\alpha$ arises because the function $\varphi_L(R)$ has resonances in the potential $V^{\text{opt}}_{\alpha}(R)$. This leads to variations of the amplitude of the function $\varphi_L$ when $Q_\alpha$ approaches the resonance energy, which in turn significantly changes the width $\Gamma_{L\sigma_f I_f}$.

Thus, although the approach proposed in Ref. 7 does eliminate from $\alpha$-decay theory the difficulty associated with choosing the parameter $R_0$, this variant of the theory has instabilities which renders the scheme impracticable for analyzing experimental data.

In this review we shall therefore consider the alternative non-$R$-matrix variant of $\alpha$-decay theory,[10,11] using it to analyze a large group of experimental data on $\alpha$ decay of spherical nuclei.

## 1. INTEGRAL EXPRESSION FOR THE $\alpha$-DECAY WIDTH

Using the results of Refs. 10–13, we shall derive systematically an integral expression for the $\alpha$-decay width. We shall restrict ourselves to the case when only $\alpha$-particle channels are open. Then, in the case of narrow widths, the state of an $\alpha$-decay nucleus $A$ can be described by a quasistationary wave function $\Psi^{I_i M_i}_{\sigma_i}$ with complex energy $E_0 - i\Gamma/2$, with the asymptotic behavior

$$\Psi^{I_i M_i}_{\sigma_i} \to \sum_{L\sigma_f I_f} C_{L\sigma_f I_f} u^{I_i M_i}_{L\sigma_f I_f} \frac{1}{R}[G_L(R) + iF_L(R)] \exp(i\beta^{\text{pot}}_{L\sigma_f I_f}), \tag{11}$$

where $\beta^{\text{pot}}_{L\sigma_f I_f}$ is the nuclear potential phase shift in the channel $L\sigma_f I_f$; $F_L$ and $G_L$ are, respectively, the regular and irregular Coulomb radial function having, respectively, sine and cosine asymptotic behavior

$$F_L(R) \to \sin(kR - L\pi/2 + \beta^{\text{Coul}}_L),$$

where $k = \sqrt{2mQ_\alpha/\hbar^2}$ and $\beta^{\text{Coul}}_L$ is the Coulomb phase shift. The channel function $u^{I_i M_i}_{L\sigma_f I_f}$ has already been defined by Eq. (3). Using the continuity equation, which leads to the following relation between the total width $\Gamma$ and the total probability flux:

$$\Gamma = \sum_{L\sigma_f I_f} C^2_{L\sigma_f I_f} k\hbar^2/m, \tag{12}$$

we obtain

$$C_{L\sigma_f I_f} = \sqrt{\Gamma_{L\sigma_f I_f} k/2Q_\alpha}.$$

In the case of deeply sub-barrier $\alpha$ decay, the low penetration factor of the Coulomb barrier has the consequence that

$$|\beta^{\text{pot}}_{L\sigma_f I_f}| \ll 1. \tag{13}$$

Let $R_1$ be a point to the left of and near the outer Coulomb turning point, where the condition $G_L(R_1) \gg F_L(R_1)$ already holds. Then in the asymptotic region for $R \leq R_1$ with allowance for the condition (13),

$$\Psi^{I_i M_i}_{\sigma_i} \to \sum_{L\sigma_f I_f} \sqrt{\Gamma_{L\sigma_f I_f} k/2Q_\alpha}\, u^{I_i M_i}_{L\sigma_f I_f} \frac{G_L(R)}{R}. \tag{14}$$

Note that the function $\Psi^{I_i M_i}_{\sigma_i}$ in (14) for $F_L \ll G_L$ coincides with the interior basis function $X^{I_i M_i}_{\lambda}$ used in the $R$-matrix approach to describe an isolated resonance[5]; for by its definition[5] the function $X^{I_i M_i}_{\lambda}$, like the function $\Psi^{I_i M_i}_{\sigma_i}$, is normalized to unity in the region $0 \geq R \leq R_1$ and for $R \lesssim R_1$ has the form

$$X^{I_i M_i}_{\sigma_i} \to \left(\frac{2mR}{\hbar^2}\right)^{1/2} \sum_{L\sigma_f L\sigma_f} \gamma_{\lambda I_f}(R)\, u^{I_i M_i}_{L\sigma_f I_f} \equiv \sum_{L\sigma_f I_f} u^{I_i M_i}_{L\sigma_f I_f} \frac{1}{R} \varphi_{\lambda L\sigma_f I_f}(R). \tag{15}$$

As boundary condition for the radial function $\varphi_{\lambda L\sigma_f I_f}(R)$ in the $R$-matrix scheme one usually uses the natural boundary condition for $R_0 \lesssim R_1$:

$$\left.\frac{\varphi'_{\lambda L\sigma_f I_f}}{\varphi_{\lambda L\sigma_f I_f}}\right|_{R=R_0} = \left.\frac{F_L F'_L + G_L G'_L}{F_L^2 + G_L^2}\right|_{R=R_0} \to \left.\frac{G'_L}{G_L}\right|_{R=R_0},$$

which agrees with the boundary condition for the radial part of the function $\Psi^{I_i M_i}_{\sigma_i}$.

Finally, as follows from a comparison of Eqs. (14) and (15), the partial width $\Gamma_{L\sigma_f I_f}$ can be expressed in terms of the reduced width $\gamma_{\lambda L\sigma_f I_f}$ by the ordinary $R$-matrix expression

$$\Gamma_{L\sigma_f I_f} = \frac{2kR_0}{G_L^2(R_0)} \gamma^2_{\lambda L\sigma_f I_f}(R_0) = 2P_L \gamma^2_{\lambda L\sigma_f I_f}. \tag{16}$$

We now consider the inverse of the $\alpha$-decay problem in which an $\alpha$ particle with orbital angular momentum $L^0$ is scattered on the daughter nucleus $(A-4)$ in the state $I_f^0 \sigma_f^0$, the total energy of the system being near the energy $E_0$ of the $\alpha$-decay nucleus $A$. Then the scattering wave function $\Phi^{I_i M_i}_{\sigma_i}$ in the asymptotic region has the form

$$\Phi^{I_i M_i}_{\sigma_i} \to \sum_{L\sigma_f I_f} \frac{i}{2} \{[\tilde{G}_L(R) - i\tilde{F}_L(R)]\, \delta_{\sigma_i \sigma_f^0} \delta_{LL^0} \delta_{I_f I_f^0} - S_{L\sigma_f I_f, L^0\sigma_f^0 I_f^0} [\tilde{G}_L(R) + i\tilde{F}_L(R)]\} u^{I_i M_i}_{L\sigma_f I_f}, \tag{17}$$

where $\tilde{F}_L$ and $\tilde{G}_L$ are related, respectively, to the regular and irregular radial Coulomb functions and are normalized to a $\delta$ function with respect to the energy:

$$\tilde{F}_L(R) = \sqrt{k/\pi Q_\alpha}\, F_L(R)/R. \tag{18}$$

In Eq. (17), $S_{L\sigma_f I_f, L^0\sigma_f^0 I_f^0}$ is the $S$-matrix element, which for the case of an isolated resonance has the form[5]

$$S_{L\sigma_f I_f, L^0\sigma_f^0 I_f^0} = \exp(2i\beta^{\text{pot}}_{L\sigma_f I_f})\, \delta_{LL^0} \delta_{\sigma_f \sigma_f^0} \delta_{I_f I_f^0} - \frac{\exp[i(\beta^{\text{pot}}_{L\sigma_f I_f} + \beta^{\text{pot}}_{L^0\sigma_f^0 I_f^0})] \sqrt{\Gamma_{L\sigma_f I_f}} \sqrt{\Gamma_{L^0\sigma_f^0 I_f^0}}}{E_0 - \Delta(E) - E + i\Gamma/2}, \tag{19}$$

where $\Delta(E)$ is the known shift of the level. Then in the asymptotic region for $R \lesssim R_1$ the function $\Phi^{I_i M_i}_{\sigma_i}$ in (17) can be rewritten with allowance for the condition (13) in the form

$$\Phi^{I_i M_i}_{\sigma_i} \to \sum_{L\sigma_f I_f} \frac{\tilde{G}(R)}{2} \cdot \frac{\sqrt{\Gamma_{L\sigma_f I_f}} \sqrt{\Gamma_{L^0\sigma_f^0 I_f^0}}}{E - E_0 - \Delta(E) + i\Gamma/2} u^{I_i M_i}_{L\sigma_f I_f}. \tag{20}$$

Comparison of (20) and (14) shows that the functions $\Phi^{I_i M_i}_{\sigma_i}$ and $\Psi^{I_i M_i}_{\sigma_i}$ in the asymptotic region for $R \lesssim R_1$ are identical to within a constant factor. Since these two functions satisfy the same Schrödinger equation, and as we have seen above, the boundary conditions for them in the asymptotic region $(R \approx R_1)$ are the same, in the whole of the interior region $0 \leq R \leq R_1$ we have

$$\Phi^{I_i M_i}_{\sigma_i} = \sqrt{\frac{\Gamma_{L^0\sigma_f^0 I_f^0}}{2\pi}} \cdot \frac{1}{E - E_0 - \Delta(E) + i\Gamma/2} \Psi^{I_i M_i}_{\sigma_i}. \tag{21}$$

Since, as we have already noted, the function $\Psi^{I_i M_i}_{\sigma_i}$ coincides with the function $X^{I_i M_i}_{\lambda}$, Eq. (21) is, except for the notation, exactly equivalent to the relation known in $R$-matrix theory between the scattering function and the interior function $X^{I_i M_i}_{\lambda}$ in the approximation of an isolated resonance.[5]

For the $S$ matrix we now use the expression[14]

$$S_{L\sigma_f I_f, L^0\sigma_f^0 I_f^0} = \delta_{LL^0} \delta_{\sigma_f \sigma_f^0} \delta_{I_f I_f^0} - 2\pi i \langle \tilde{F}_L u^{I_i M_i}_{L\sigma_f I_f} | \tilde{V}_{\alpha A-4} | \Phi^{I_i M_i}_{\sigma_i} \rangle, \tag{22}$$

where $\tilde{V}_{\alpha A-4}$ is the nuclear potential of the interaction between the $\alpha$ particle and the daughter nucleus, which has the form

$$\tilde{V}_{\alpha A-4} = \sum_{i=1}^{4} \sum_{j=5}^{A} V_{ij}, \tag{23}$$

where $V_{ij}$ is the potential of the nucleon pairing interaction. Comparing then (22) and (19) and using (21), and also the condition (13), we obtain the following basic expression for the $\alpha$-decay partial width:

$$\Gamma_{L\sigma_f I_f} = 2\pi |\langle \tilde{F} u^{I_i M_i}_{L\sigma_f I_f} | \tilde{V}_{\alpha A-4} | \Psi^{I_i M_i}_{\sigma_i} \rangle|^2. \tag{24}$$

In deriving Eq. (24) we have ignored antisymmetrization in the final $\alpha$-decay channel. With allowance for it,[15] Eq. (24) becomes

$$\Gamma_{L\sigma_f I_f} = 2\pi |\langle \mathcal{A}\{\tilde{F}_L u^{I_i M_i}_{L\sigma_f I_f} | \tilde{V}_{\alpha A-4}\} | \Psi^{I_i M_i}_{\sigma_i} \rangle|^2, \tag{25}$$

where $\mathcal{A}$ is the antisymmetrization operator. Equation (25) is rigorous. Of course, actual calculations require the introduction of certain approximations for all the many-particle functions in (25). Below, we shall investigate the possibility of analyzing the $\alpha$ widths by means of Eq. (25) in the framework of the shell model for spherical nuclei. In addition, we shall study $\alpha$ decay on the basis of Eq. (25), making use of the notion of $\alpha$ clustering.

## 2. ALPHA DECAY IN THE SHELL MODEL

*Width of $\alpha$ Decay of Spherical Nuclei.* We shall restrict ourselves below to considering the case when the main contribution to the $\alpha$-decay width is due to the wave-function component of the parent nucleus $A$ which corresponds to the motion of four nucleons forming an

$\alpha$ particle above a core identical with the daughter nucleus $A-4$ (diagonal approximation). Then, using the Green's function method,[9,18] we can transform the potential $\tilde{V}_{\alpha A-4}$ in Eq. (25) to the form

$$\bar{V}_{\alpha A-4} = \sum_{i=1}^{4} V_i + \sum_{i<j=1}^{4} (\Gamma_{ij} - V_{ij}), \tag{26}$$

where $V_i$ is the real part of the nucleon optical potential, equal at low energies to the shell potential [see Eq. (9)].

In Eq. (26), $\Gamma_{ij}$ is a four-pole irreducible with respect to the particle-particle channel and has the meaning of the effective interaction potential between the nucleons in the parent nucleus.[17] There are weighty arguments indicating that the effective interaction of nucleons within a nucleus differs from their interaction in vacuum. In this case, the second term in Eq. (26) has a three-dimensional character and in order of magnitude may be comparable with the first term.[18] However, since reliable information about the properties of $\Gamma_{ij}$ is currently unavailable, in the first approximation we shall ignore the second term in the interaction $\bar{V}_{\alpha A-4}$ in (26).

It would appear that significant destructive interference of the first and second terms in (26) is improbable because of their different natures, so that allowance in (26) for terms with renormalization of the interaction should not lead to a significant change of the $\alpha$ widths. Thus, the potential of the interaction between the $\alpha$ particle and the daughter nucleus used in the calculations is the same as the potential (9) introduced earlier in Ref. 7.

Note that in Ref. 19 Săndulescu generalizes Harada and Rauscher's expression (8) for the $\alpha$-decay width to the case when the second term in the interaction $\bar{V}_{\alpha A-4}$ in (26) is taken into account. He assumes that $V_\alpha^{\text{opt}}(R)$ is equal to the first term of Eq. (26), and this, according to his argument, is equivalent to the vanishing of the matrix element (8). Then the interaction responsible for $\alpha$ decay is the second term in (26). However, in accordance with the results of Ref. 18, the potential $V_\alpha^{\text{opt}}(R)$ must be equal in the diagonal approximation to the total potential $\bar{V}_{\alpha A-4}$ from (26). This renders the conclusions of Ref. 19 selfcontradictory.

We now face the problem of particularizing the general expression (25) for the $\alpha$ width. We assume that the wave functions of the parent and daughter nuclei can be represented in the form[16]

$$\Psi_{\sigma_i \text{i.sh.}}^{I_i M_i} = \sum_{P_i N_i} |(P_i N_i)\, I_i M_i\rangle \langle P_i N_i \| i\rangle; \tag{27}$$

$$\Psi_{\sigma_f \text{f.sh}}^{I_f M_f} = \sum_{P_f N_f} |(P_f N_f)\, I_f M_f\rangle \langle P_f N_f \| f\rangle, \tag{28}$$

where $P_i$ and $N_i$ are, respectively, the states of the proton and neutron system in the simple shell model with the same number of protons and neutrons, respectively, as in the parent nucleus; $\langle P_i N_i \| i\rangle$ and $\langle P_f N_f \| f\rangle$ are the configuration-mixing coefficients. Substituting the functions (27) and (28) into (25) and then following the arguments of Ref. 16, we obtain the following expression for the integrated $\alpha$-decay width:

$$\Gamma_{L\sigma_f I_f} = 2\pi \left| \int \Theta_{L\sigma_f I_f}(R)\, \tilde{F}_L(R)\, R^2\, dR \right|^2, \tag{29}$$

where the complete overlap integral $\Theta_{L\sigma_f I_f}$ is given by

$$\begin{aligned}
\Theta_{L\sigma_f I_f}(R) = {} & \sum_{\substack{P_i N_i P_f N_f \\ P_\alpha N_\alpha}} \hat{J}_{P_i} \hat{J}_{N_i} \hat{I}_f J_{P_\alpha} J_{N_\alpha} \\
& \times \prod_{i=1}^{4} \hat{j}_i \sqrt{2-\delta_{n_1 n_2}\delta_{l_1 l_2}\delta_{j_1 j_2}}\, \sqrt{2-\delta_{n_3 n_4}\delta_{l_3 l_4}\delta_{j_3 j_4}} \\
& \times \begin{Bmatrix} J_{P_f} & J_{N_f} & I_f \\ J_{P_\alpha} & J_{N_\alpha} & L \\ J_{P_i} & J_{N_i} & I_i \end{Bmatrix} \begin{Bmatrix} l_1 & 1/2 & j_1 \\ l_2 & 1/2 & j_2 \\ J_{P_\alpha} & 0 & J_{P_\alpha} \end{Bmatrix} \begin{Bmatrix} l_3 & 1/2 & j_3 \\ l_4 & 1/2 & j_4 \\ J_{N_\alpha} & 0 & J_{N_\alpha} \end{Bmatrix} \\
& \times \langle P_f P_\alpha \| P_i\rangle \langle N_f N_\alpha \| N_i\rangle \langle P_i N_i \| i\rangle \langle P_f N_f \| f\rangle \\
\times \int \mathcal{A} & \{\chi_\alpha(\xi_1, \xi_2, \xi_3)\, S_\alpha(1, 2, 3, 4)\, V_{\alpha A-4}(\mathbf{r}_1, \mathbf{r}_2, \mathbf{r}_3, \mathbf{r}_4)\, Y_{LM}(\Omega_R)\} \\
& \times [[\psi_{n_1 l_1 j_1}(\mathbf{r}_1)\, \psi_{n_2 l_2 j_2}(\mathbf{r}_2)]_{J_{P_\alpha}} [\psi_{n_3 l_3 j_3}(\mathbf{r}_3)\, \psi_{n_4 l_4 j_4}(\mathbf{r}_4)]_{J_{N_\alpha}}]_{LM} \\
& \times D\, d\xi_1\, d\xi_2\, d\xi_3\, d\Omega_{\mathbf{R}},
\end{aligned} \tag{30}$$

where $\hat{J} = \sqrt{2J+1}$; $\langle P_f P_\alpha \| P_i\rangle$ and $\langle N_f N_\alpha \| N_i\rangle$ are the fractional parentage coefficients for separating two protons with angular momentum $J_{P_\alpha}$ from the states $(n_1 l_1 j_1)$ and $(n_2 l_2 j_2)$ and two neutrons with the angular momentum $J_{N_\alpha}$ from the states $(n_3 l_3 j_3)$ and $(n_4 l_4 j_4)$; $\psi_{n_i l_i j_i}(\mathbf{r}_i)$ is the shell wave function of nucleon $i$; $D = 8$ is the Jacobian of the transition from the variables $\mathbf{r}_1$, $\mathbf{r}_2$, $\mathbf{r}_3$, $\mathbf{r}_4$ to the variables $\xi_1$, $\xi_2$, $\xi_3$, $\mathbf{R}$ (6). In Eq. (30), the notation $[\psi_{n_1 l_1 j_1}\psi_{n_2 l_2 j_2}]_{J_{P_\alpha}}[\psi_{n_3 l_3 j_3}\psi_{n_4 l_4 j_4}]_{J_{N_\alpha}}]_{LM}$ determines the scheme for adding the angular momenta of the four nucleons which form the $\alpha$ particle.

Note that in Eq. (29) there is no free parameter, for the wave functions of the parent and the daughter nucleus are taken from shell calculations with allowance for configuration mixing, the parameters of the potential $V_{\alpha A-4}$ in (9) are fixed in the same calculations, and the parameters of the interior wave function $\chi_\alpha$ of the $\alpha$ particle are determined experimentally from fast-electron scattering on $^4$He. Below, the function $\chi_\alpha$ is used in the simplest form (5), although in principle the methods developed also enable one to take into account the more complicated components of this function which were investigated, for example, in Ref. 20. The absence in Eq. (29) of fitting parameters peculiar to $\alpha$ decay means that the results of calculations can be compared almost unambiguously with experiments in this approach.

*Method of Calculating Overlap Integrals.* The main difficulty in obtaining $\alpha$ widths by means of Eq. (29) is the calculation of the multidimensional overlap integrals $\Theta_{L\sigma_f I_f}(R)$. Until recently, they and the related quantities $\gamma_{l\sigma_f L_f}$ in (2) had been consistently calculated only with the use of oscillator shell basis, for which the multidimensional integration is reduced to one-dimensional integration[4,22] by means of Talmi-Moshinsky transformations.[21] In this review we use the overlap integrals $\Theta_{L\sigma_f I_f}(R)$ calculated for realistic wave functions by the method proposed in Ref. 23.

It is helpful to compare the properties of the overlap integrals obtained using the Woods-Saxon basis $\Theta^{\text{WS}}_{L\sigma_f I_f}$ and the oscillator basis $\Theta^{\text{os}}_{L\sigma_f I_f}$. As can be seen from Fig. 1, $\Theta^{\text{WS}}_{L\sigma_f I_f}(R)$ (curve 1) and $\Theta^{\text{os}}_{L\sigma_f I_f}$ (curve 2) in the interior region are close to one another and have the same number of nodes. However, on the surface of

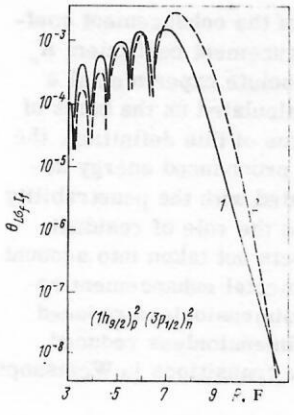


FIG. 1. Overlap integrals $\Theta_{L\sigma_f I_f}(R)$ for $^{210}$Po (configuration $[[1h_{9/2}1h_{9/2}]_0 \times [3p_{1/2}3p_{1/2}]_0]_{00}$): 1) with shell wave functions of the Woods-Saxon potential; 2) for harmonic-oscillator potential.

the nucleus they differ strongly, which reduces the absolute widths $\Gamma^{WS}_{L\sigma_f I_f}$ calculated by (29) for simple shell configurations by from 5 to 30 times compared with $\Gamma^{os}_{L\sigma_f I_f}$, depending on the type of configuration.

In contrast to the $R$-matrix theory of $\alpha$ decay, in the present approach the overlap integral $\Theta_{L\sigma_f I_f}(R)$ contains the potential (9), which depends not only on the coordinates $\mathbf{R}$ of the center of mass of the $\alpha$ particle but also on its internal variables $\xi_1$, $\xi_2$, $\xi_3$. Since this last circumstance greatly complicates the calculations, it is helpful to clarify the contribution of the $\xi$ dependence of $V_{\alpha A-4}$ to the $\alpha$-decay width $\Gamma_{L\sigma_f I_f}$. In Table 1 we give typical ratios $(\Gamma_{L\sigma_f I_f} - \Gamma^0_{L\sigma_f I_f})/\Gamma_{L\sigma_f I_f}$, where $\Gamma^0_{L\sigma_f I_f}$ is the width calculated in the approximation

$$V_{\alpha A-4} = \sum_{i=1}^{4} V_i(|\mathbf{r}_i|) = \sum_{i=1}^{4} V_i(R) \equiv V_{\alpha A-4}(R) \qquad (31)$$

for the example of the shell configuration $[(1h_{9/2})^2_{J_{P_\alpha}} \times (2g_{9/2})^2_{J_{N_\alpha}}]_{LM}$ of the $^{210}$Po nucleus. It can be seen that the effect of the $\xi$ dependence of the potential $V_{\alpha A-4}$ is small and changes little with increasing angular momentum $L$ of the emitted $\alpha$ particle. Then in the approximation (31) the overlap integral $\Theta_{L\sigma_f I_f}$ can be represented in the form

$$\Theta_{L\sigma_f I_f}(R) = V_{\alpha A-4}(R)\,\Psi_{L\sigma_f I_f}(R)/R; \qquad (32)$$

where

$$\Psi_{L\sigma_f I_f}(R) \equiv \langle \Psi^{I_i M_i}_{\sigma_i} | u^{I_f M_f}_{L\sigma_f I_f} \rangle R \qquad (33)$$

is the effective wave function of the center of mass of the four nucleons forming the $\alpha$ particle. In the language of this function, Eq. (25) for the $\alpha$-decay width takes the "one-particle" form

$$\Gamma_{L\sigma_f I_f} = 2\pi \left| \int \Psi_{L\sigma_f I_f}(R)\, V_{\alpha A-4}(R)\, \tilde{F}_0(R)\, R\, dR \right|^2. \qquad (34)$$

The previously introduced amplitude $\gamma_{L\sigma_f I_f}(R)$ (2) of the reduced width can be expressed in terms of $\Psi_{L\sigma_f I_f}(R)$ by the relation

$$\gamma_{L\sigma_f I_f}(R) = \sqrt{\hbar^2/2mR}\,\Psi_{L\sigma_f I_f}(R). \qquad (35)$$

TABLE 1.

| $L$ | 0 | 2 | 4 | 6 | 8 | 10 | 12 | 14 | 16 |
|---|---|---|---|---|---|---|---|---|---|
| $\frac{\Gamma_{L\sigma_f I_f} - \Gamma^0_{L\sigma_f I_f}}{\Gamma_{L\sigma_f I_f}}$, % | 12 | 11.3 | 12.9 | 12.7 | 13.3 | 14.9 | 16.5 | 18.1 | 20 |

TABLE 2.

| Parent nucleus | Configuration $[(lj)^3_{J_{P_\alpha}}(lj)^3_{J_{N_\alpha}}]_{LM}$ | $\lg\left(\frac{\Gamma_{L\sigma_f I_f}}{\Gamma^{pnt}_{L\sigma_f I_f}}\right)$ | $\lg\left(\frac{B_{os}}{B_{sw}}\right)$ |
|---|---|---|---|
| $^{210}$Po | $[(1h_{9/2})^2_0 (3p_{1/2})^2_0]_{00}$ | −2.24 | 0.16 |
| $^{208}$Po | $[(1h_{9/2})^2_0 (3p_{3/2})^2_0]_{00}$ | −2.26 | 0.16 |
| $^{206}$Po | $[(1h_{9/2})^2_0 (2f_{5/2})^2_0]_{00}$ | −2.78 | 0.36 |
| $^{212}$Po | $[(1h_{9/2})^2_0 (2g_{9/2})^2_0]_{00}$ | −2.78 | 0.24 |
| $^{226}$Ra | $[(1h_{9/2})^2_0 (1i_{11/2})^2_0]_{00}$ | −3.85 | 0.65 |
| $^{196}$Po | $[(1h_{9/2})^2_0 (1i_{13/2})^2_0]_{00}$ | −4.00 | 0.58 |
| $^{200}$Rn | $[(1h_{9/2})^2_0 (1i_{13/2})^2_0]_{00}$ | −3.97 | 0.60 |
| $^{180}$Hg | $[(2d_{5/2})^2_0 (1h_{9/2})^2_0]_{00}$ | −2.82 | 0.38 |
| $^{174}$Pt | $[(2d_{5/2})^2_0 (1h_{9/2})^2_0]_{00}$ | −2.83 | 0.35 |
| $^{186}$Pt | $[(2d_{5/2})^2_0 (1i_{13/2})^2_0]_{00}$ | −3.18 | 0.44 |

Note that the calculation of the widths $\Gamma^{pnt}_{L\sigma_f I_f}$ in the approximation of a point $\alpha$ particle ($\mathbf{r}_1 = \mathbf{r}_2 = \mathbf{r}_3 = \mathbf{r}_4 = \mathbf{R}$) is much more economic than calculations which take into account the finite size of the $\alpha$ particle. However, this approximation is realistic for neither the relative nor the absolute $\alpha$-decay widths. Nevertheless, if one does introduce

$$B = \Gamma_{L\sigma_f I_f}/\Gamma^{pnt}_{L\sigma_f I_f}, \qquad (36)$$

it is possible to make calculations in the point approximation using the ratio $B$ as a correcting factor,[1] which takes into account the finite size of the $\alpha$ particle.

Typical values of the correcting factors $B$ are given in the third column of Table 2. They vary from 250 to $1 \cdot 10^4$ and depend strongly on the particular shell configurations of the nucleons forming the $\alpha$ particle.

*Comparison with the R-Matrix Variant.* If Eqs. (35) and (34) are used, the $\alpha$ width in the present approach can be represented in the form

$$\Gamma_{L\sigma_f I_f} = \frac{4\pi m}{\hbar^2} \left| \int \gamma_{L\sigma_f I_f}(R)\, V_{\alpha A-4}(R)\, \tilde{F}_L(R)\, (R)^{3/2}\, dR \right|^2. \qquad (37)$$

The integrand in Eq. (37) peaks at a point $R_m$ in the surface region of the nucleus. This peak arises because the amplitude of the reduced width $\gamma_{L\sigma_f I_f}(R)$ and the potential $V_{\alpha A-4}(R)$ decrease exponentially in the exterior region, whereas the Coulomb function $\tilde{F}_L(R)$ is exponentially damped in the interior region. The formation of this peak in the case of $^{210}$Po is shown in Fig. 2. The effective width $b$ of the peak can be estimated if the value of the integral in (37) is divided by the value of the integrand at the point $R_m$. Numerical calculations give 1.5—1.8 F for $b$. Then Eq. (37) can be represented approximately in the form

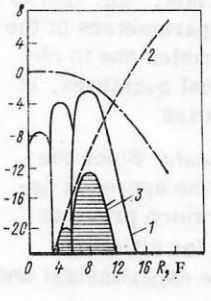


FIG. 2. Formation of a maximum in the integrand of the expression (29) for the $\alpha$ width: 1) logarithms of the modulus of the overlap integral $\Theta^{(R)}_{L\sigma_f I_f}$; 2) logarithm of the function $F_L(R)$; 3) logarithm of the modulus of the integrand, and the width of principal maximum of the hatched figure determines $b$ in Eq. (38).

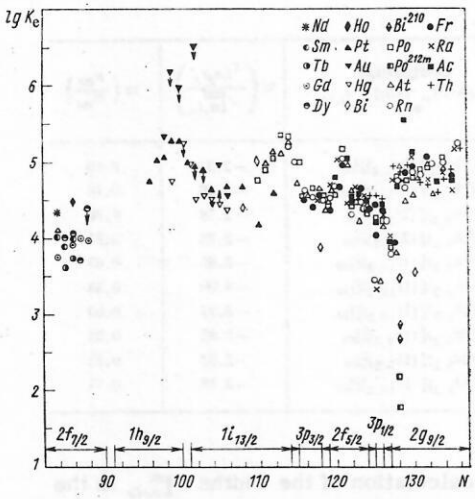


FIG. 3. Logarithms of experimental enhancement factors as a function of the neutron number $N$. The neutron shell configurations for which the calculation was made are shown along the abscissa.

$$\Gamma_{L\sigma_f I_f} = \frac{2\pi R_m}{Q_\alpha} |kbV_{\alpha A-4}(R_m) \tilde{F}_L(R_m) \gamma_{L\sigma_f I_f}(R_m)|^2. \quad (38)$$

Comparison of Eq. (38) with the $R$-matrix expression for the width (1) shows that $R_m$ corresponds to the effective cutoff radius $R_0$. Concrete calculations show that $R_m$ for different nuclei is in the region of the range of the shell potential $R_A$ ($\approx 7.5$ F for $^{210}$Po), whereas in the traditional calculations $R_0$ is as a rule chosen to the right of the inner Coulomb turning point ($R_0 > 9.5$ F for $^{210}$Po). The effective penetration factor in the given scheme is

$$P_L^{\text{eff}}(R_m) = kR_m \frac{\pi k}{Q_\alpha} |bV_{\alpha A-4}(R_m) \tilde{F}_L(R_m)|^2. \quad (39)$$

Estimates show[24] that in the majority of interesting cases $P_L^{\text{eff}}(R_m)$ is about 100 times larger than the Thomas penetration factor taken at the point $R_m$. At the same time, the dependences of $P_L^{\text{eff}}$ on $Q_\alpha$ and $L$ remain practically the same as in the usually adopted variants of $\alpha$-decay theory. Detailed investigations show that $R_m$ fluctuates significantly ($\Delta R_m \approx 0.5$ F) depending on the types of the shell states of the four nucleons forming the $\alpha$ particle. Therefore, the effective penetration factor depends on the state of the nucleons through $R_m$ and is not an universal function, as was assumed in Refs. 3 and 4 This result makes it doubtful whether one can use a single penetration factor for different types of states of the four nucleons, especially in calculations with configuration mixing.

In contrast to the expressions (1) of the $R$-matrix theory and Harada and Rauscher's variant,[8] Eq. (29) is stable against small variations of the parameters of the potential and wave functions, which enables one to obtain reliable values of all the theoretical quantities, including the absolute $\alpha$-decay probabilities.

*Experimental Enhancement Coefficients*. Since the reduced width is related integrally in the approach developed here to the absolute $\alpha$ width, which prevents one using a single effective radius $R_m$ for different states, it is convenient to compare the experimental and theoretical $\alpha$ widths by means of the enhancement coefficients. The experimental enhancement coefficient $K_e$ is defined as the ratio of the absolute experimental $\alpha$ width to the theoretical width calculated on the basis of the simple shell model. By virtue of this definition, the coefficient does not include the pronounced energy dependence of the $\alpha$ width associated with the penetrability of the barrier and characterizes the role of residual interactions and also other effects not taken into account in the shell model. The experimental enhancement coefficients are analogous to the dimensionless reduced widths in Wigner units or the dimensionless reduced probabilities of electromagnetic transitions in Weisskopf units.

Figure 3 shows the logarithms of the experimental enhancement coefficients calculated with parameters of the shell potential from Ref. 59 for a large group of doubly even, odd, and doubly odd spherical nuclei ($144 \leq A \leq 235$) as a function of the neutron number. A detailed bibliography of papers in which experimental $\alpha$ widths are reported for these nuclei can be found in Refs. 26 and 63.

The most numerous group of nuclei in Fig. 3 corresponds to the favored $\alpha$ decay when the emitted $\alpha$ particle is formed from nucleons paired with zero angular momentum; this group has $L = 0$. The values of $\lg K_e$ for this group of nuclei lie in the range $4.2 \leq \lg K_e \leq 5.3$. The overwhelming majority of nuclei of this group lie in a narrow strip of width $\lg K_e \leq 0.6$, while the neighboring even and odd nuclei have similar enhancement coefficients.

Since the proximity of the enhancement coefficients $K_e$ of neighboring nuclei for favored $\alpha$ transitions is an experimental tendency, as can be seen from Fig. 3, strong deviations of the experimental enhancement coefficients for any nucleus from the coefficients $K_e$ for neighboring nuclei indicate either unreliability of the experimental data or that the $\alpha$ transition is not favored (in the case of a deviation downward of $K_e$ from the values of $K_e$ for the neighboring nuclei). For some investigated odd and doubly odd nuclei the experimental enhancement coefficients were appreciably larger than those for the neighboring doubly even nuclei, which indicates the unreliability of the experimental data and enables one to predict a region of probable values of the corresponding widths. For a number of isotopes of Ir, Pt, Po, Fr, At, Ac, theoretical predictions of this kind are given in Table 3.

The second group of nuclei is formed by isotopes with $N = 125$ and 127 and also odd isotopes of Bi with $Z = 83$. For $\alpha$ decays in these nuclei, one of the pair of nucleons forming the $\alpha$ particle has nonzero total angular momentum, whereas the second pair has zero. The experimental enhancement coefficients for the nuclei of this group are significantly lower than for the favored band. The logarithms of $K_e$ lie in the range from 3.06 to 4.0.

In Fig. 3 a particular position is occupied by the $^{210}$Bi nucleus, for which the odd proton and odd neutron are above the doubly magic core of $^{208}$Pb. In Fig. 3 we give $\lg K_e$ for $\alpha$ decays from the ground state of $^{210}$Bi with

TABLE 3.

| Isotope | Branching ratios or $T^{\alpha}_{1/2}$ | | |
|---|---|---|---|
| | Experiment, 1972 | Theoretical predictions, 1972 | Experiment, 1974 |
| $^{171}$Ir — $^{173}$Ir | ? | $\sim 1.0$ | — |
| $^{174}$Ir | ? | $\sim 0.25$ | — |
| $^{175}$Ir | ? | $\sim 0.1$ | — |
| $^{176}$Ir — $^{177}$Ir | ? | $\sim 0.01$ | — |
| $^{181}$Pt | $6\cdot10^{-4}$ | $\sim 3\cdot10^{-4}$ | — |
| $^{183}$Pt | $10^{-5}$ | $\sim 10^{4}$ | — |
| $^{192}$Pt | $T^{\alpha}_{1/2}=10^{15}$ years | $T^{\alpha}_{1/2}\approx 10^{18}$ years | — |
| $^{203}$Po | ? | $\sim 0.01$ | 0.002 |
| $^{217}$Po | $T^{\alpha}_{\alpha/2}<10$ sec | $T^{\alpha}_{1/2}\sim 1.25$ sec | — |
| $^{204}$Fr | ? | $\sim 1.0$ | 0.7 |
| $^{205}$Fr | ? | $\sim 1.0$ | 0.97 |
| $^{206}$Fr | ? | $\sim 1.0$ | 0.85 |
| $^{207}$Fr | ? | $\sim 1.0$ | 0.93 |
| $^{208}$Fr | ? | $\sim 1.0$ | 0.74 |
| $^{209}$Fr | ? | $\sim 1.0$ | 0.89 |
| $^{200}$At | ? | $\sim 1.0$ | 0.32 |
| $^{201}$At | ? | $\sim 1.0$ | 0.71 |
| $^{218}$Ac | $T^{\alpha}_{1/2}=2.7\times10^{-7}$ sec | $T^{\alpha}_{1/2}=1.26\times10^{-6}$ | — |

$I_i^{\pi i}=1^-$ to the first ($I_f^{\pi f}=2^-$, lower point) and second ($I_f^{\pi f}=1^-$, upper point) excited states of the daughter nucleus $^{206}$Tl.

For both decays, the $\alpha$ particle is formed from two pairs of unpaired nucleons. The $\lg K_e$ values for $^{210}$Bi lie lower than those of the second group of nuclei and are about 2.7.

Thus, as follows from Fig. 3, the ratios of the experimental and theoretical $\alpha$ widths calculated in the shell model without configuration mixing vary in the wide range from $4.5\cdot10^2$ to $2\cdot10^5$, which demonstrates the impossibility of explaining the absolute $\alpha$-decay probabilities on the basis of this model. The nonmonotonicity in the behavior of the experimental enhancement coefficients as a function of the neutron number also indicates the impossibility of describing the relative variation of the experimental $\alpha$ widths of that model.

*Calculations of $\alpha$ Widths with Configuration Mixing for the Isomer $^{121m}$Po and the Nucleus $^{210}$Bi.* We now turn from the simple shell model to models which take into account nucleon-nucleon correlations. In the investigated region of nuclei, because of the fundamental computational difficulties, diagonalization calculations can be carried out consistently only for nuclei in the immediate proximity of the doubly magic nucleus $^{208}$Pb.

In this connection, particular interest attaches to an $\alpha$-decay investigation of the isomer $^{212m}$Po ($I_i^{\pi i}=18^+$), whose high spin requires almost complete alignment of the shell angular momenta of the outer nucleons, which greatly reduces the number of important components in the shell diagonalization basis. In addition, this scheme of adding angular momenta automatically eliminates the contribution of pairing effects. All this gives one reason to hope that the shell wave function obtained for the isomeric state with $I_i^{\pi i}=18^+$ by diagonalization is fairly accurate. Below, in the calculations we use the wave functions of the $^{212m}$Po and $^{208}$Pb nuclei from Refs. 27 and 28. The doubly odd nucleus $^{210}$Bi is as convenient for investigation as $^{212m}$Po. In its case, the shell structure of the parent and daughter nuclei is fairly simple and there are no pairing effects. The wave functions of $^{210}$Bi and $^{206}$Tl used in the calculations are taken from Refs. 29 and 30.

It follows from the results of the calculations (Table 4) that for the $\alpha$ decay of $^{212m}$Po and $^{210}$Bi the theory reproduces reasonably the experimental relative widths. However, the theoretical absolute $\alpha$-decay probabilities are about two orders of magnitude lower than the experimental. Since there is no pairing in these nuclei and the diagonalization procedure leads to fairly reliable functions, this last result can serve as a test of the possibilities of the shell model with configuration mixing and gives an estimate of the limiting level of agreement with experiments in this model.

*$\alpha$ Decay of Spherical Nuclei in a Superfluid Model.* As we have already noted, for nuclei of the first and second groups (see Fig. 3) at least one of the two pairs of nucleons forming the $\alpha$ particle has zero total angular momentum. Therefore, the $\alpha$ decay of these nuclei cannot be described without taking into account pairing effects. The most consistent model, specially adapted for studying such effects, is the superfluid model of the nucleus.[31]

The importance of taking into account superfluid correlations in calculations of the absolute $\alpha$-decay probabilities was first pointed out by Solov'ev,[32] who obtained enhancement factors approximately equal to $10^3$ for the $\alpha$ decay of deformed nuclei. In Ref. 16, Zeh proved the need to take into account superfluidity if one is to understand the variation of the relative $\alpha$ widths in the case of spherical nuclei (taking as example the Po isotopes).

The $\alpha$-decay width in the superfluid model is determined by Eq. (29), in which the shell fractional parentage coefficients are replaced by the corresponding superfluid coefficients, which are obtained in Ref. 16. In the superfluid model, the neutron and proton correlations are independent. We introduce the neutron enhancement coefficient $K_n$, which is defined by the ratio of the $\alpha$ width calculated with allowance for only the neutron correlations to the $\alpha$ width obtained in the simple shell model, and the proton enhancement coefficient $K_p$, defined similarly.

The superfluid enhancement mechanism of the absolute $\alpha$-decay probabilities, which leads to the appearance of the enhancement coefficients $K_n$ and $K_p$, can be illustrated in the language of the effective wave function $\Psi^{sh\cdot sf}_{L\sigma_f I_f}$ of the center of mass of the four nucleons forming the $\alpha$ particle in the superfluid model. This function is determined by (33) and is related to the superfluid $\alpha$ width by Eq. (34). Because the Cooper pairing is coherent, the function $\Psi^{sh\cdot sf}_{L\sigma_f I_f}$ for favored $\alpha$ decays of doubly even nuclei must differ strongly from the analogous

TABLE 4.

| Parent nucleus | | Daughter nucleus | | | $\frac{\Gamma^e_\alpha}{\Gamma^{sh}_\alpha}$ |
|---|---|---|---|---|---|
| Isotopes | $I_i^{\pi i}$ | Isotopes | $E_{exc}$, MeV | $I_f^{\pi f}$ | |
| $^{210}$Bi | $1^-$ | $^{206}$Tl | 0.266 | $2^-$ | 308 |
| $^{210}$Bi | $1^-$ | $^{206}$Tl | 0.304 | $1^-$ | 365 |
| $^{212m}$Po | $18^+$ | $^{208}$Pb | 0 | $0^+$ | 25.5 |
| $^{212m}$Po | $18^+$ | $^{207}$Pb | 2.615 | $3^-$ | 36.8 |

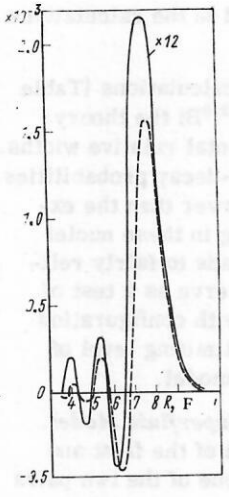


FIG. 4. Comparison of the functions $\Psi^{sh\cdot sf}_{L\sigma_f I_f}(R)$ (continuous curve and $\Psi^{sh}_{L\sigma_f I_f}(R)$ (dashed curve) for $^{216}$Ra.

function $\Psi^{sh}_{L\sigma_f I_f}$ obtained in the shell model without configuration mixing; for, as can be seen from Fig. 4, $\Psi^{sh\cdot sf}_{L\sigma_f I_f}$ has a strong peak on the surface of the nucleus, its amplitude exceeding the amplitude of the last maximum of $\Psi^{sh}_{L\sigma_f I_f}$ by a factor of about $\sqrt{K_p K_n}$.

The calculation of the superfluid $\alpha$ width with realistic nucleon shell functions is very complicated. We shall therefore discuss the effects of superfluid correlations in the simplified "hybrid" scheme proposed in Ref. 22, in which the $\alpha$ widths are calculated with realistic nucleon shell functions in the approximation of a point $\alpha$ particle and the corrections associated with the finite size of the $\alpha$ particle are introduced by means of the correcting factors $B$ in Eq. (36).

As factors $B$, we used those calculated in Ref. 22 with oscillator shell functions and corrected for the difference between the correcting factors due to the transition to the shell functions of the Woods-Saxon potential (see Table 2).

The logarithms of $K_e$ (points) and $K_{sf} = K_n K_p$ (dashed curves) calculated for the favored band are given in Fig. 5. The parameters of the superfluid model and the details of the calculations are discussed in detail in Refs. 22, 25, and 26.

As can be seen from Fig. 5, $K_{sf}$ reproduces reasonably the relative dependence of the corresponding experimental enhancement coefficients for all nuclei with developed superfluidity. At the same time, the total superfluid enhancement coefficient varies for the investigated region of nuclei from about 200 for $N \approx 106$ to 3000 for $N = 114$ and is of order $10^3$ around $N = 100$ and 134. The maximal values of the coefficients $K_{sf}$ are near the superfluid enhancement coefficients in the region of deformed nuclei ($230 \leq A \leq 254$), calculated in Ref. 32. This fact is not surprising, since the energy gaps for spherical nuclei with developed superfluidity are close to those for deformed nuclei.

As can be seen from Fig. 5, the ratio $\Gamma^{sf}_{L\sigma_f I_f}/\Gamma^{e}_{L\sigma_f I_f}$ for the regions $N < 109$ and $N > 130$ is approximately two to four times less than in the region $109 \leq N \leq 124$. Such results had been obtained earlier in Ref. 19, in which a study was made of the effect of superfluidity on the $\alpha$ decay of Po isotopes in the framework of the $R$-matrix scheme. In Ref. 19, the differences between the relative enhancement coefficients for the two regions with $N < 126$ and $N > 126$ were attributed to the increase in the importance of the $n$-$p$ correlations for the last region, these being ignored in the superfluid model. It may be that the spread of the $\Gamma^{sf}_{L\sigma_f I_f}/\Gamma^{e}_{L\sigma_f I_f}$ values is due to such a factor.

However, there is a different possibility for explaining such discrepancies if one assumes that nuclei in the regions $N < 109$ and $N > 130$ go over from a spherical to a deformed form. For this there are certain experimental indications.[45,63]

Summarizing, we may say that the dependence of the ratio $\Gamma^{e}_{L\sigma_f I_f}/\Gamma^{sf}_{L\sigma_f I_f}$ on the neutron number for favored $\alpha$ transitions is smoothed when allowance is made for superfluid correlations and it then lies in the range from 60 to 250.

For the semifavored $\alpha$ decays of isotones with $N = 125$ and 127, and also for the odd isotopes $^{213}$Bi, $^{211}$Bi, $^{201}$Bi ($Z = 83$), which are shown in Fig. 5, the superfluid enhancement coefficients are simply $K_p$ and $K_n$, respectively, since in the neutron system in the first case and the proton system in the second case, pairing is not effective. This enables one to understand the difference between the experimental enhancement coefficients of favored and semifavored decays. In Fig. 5, the dot-dash-dot curves show the dependence of the neutron superfluid enhancement coefficient $K_n(N)$ for the example of the Po isotopes. Comparing these values with the total coefficients $K_{sf} = K_p K_n$, we see that in the region $N > 110$ the proton coefficient $K_p$ is approximately constant and about ten. For the case of the odd isotopes $^{213}$Bi, $^{211}$Bi, and $^{201}$Bi the total enhancement coefficient must be near $K_n$ for Po isotopes with $N = 118$, 128 and $N = 130$ ($K \approx 16$–$40$). At the same time, for the odd isotones with $N = 125$ and 127 the enhancement coefficient must be near the $K_p$ for the corresponding doubly even isotopes ($K_p \approx 10$). The values of the neutron and proton theoretical enhancement coefficients for nuclei with $N = 126$ and $Z = 84$, in which the concepts of the superfluid model are inadequate, were obtained by the diagonalization method (see below). Thus, the ratios $\Gamma^{e}_{L\sigma_f I_f}/\Gamma^{sf}_{L\sigma_f I_f}$ for semifavored $\alpha$ decays is about 300 for nuclei with $N = 125$, about 600 for isotones with $N = 127$, and $\approx 200$ for the isotopes $^{213}$Bi, $^{201}$Bi, and $^{211}$Bi.

Finally, for nonfavored $\alpha$ decays the superfluid en-

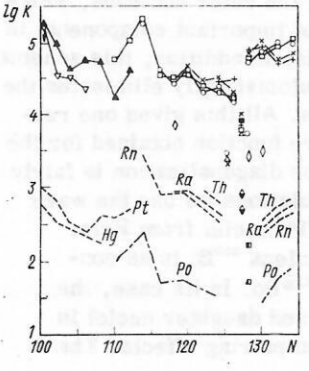


FIG. 5. Comparison of the logarithms of the experimental enhancement coefficients (points joined by continuous lines) and the superfluid enhancement coefficients (dashed lines) for favored $\alpha$ decays of doubly even nuclei with $100 \leq N \leq 134$. The notation is as in Fig. 3; --- superfluid enhancement coefficients for Po isotopes.

hancement coefficient is unity, $K_{sf}=1$, since the $\alpha$ particle is formed from a pair of neutrons and protons with nonzero angular momentum, so that $\Gamma^{e}_{L\sigma_f I_f}/\Gamma^{sf}_{L\sigma_f I_f}=K_e\approx 30-300$.

Thus, in the framework of the superfluid model one can explain the experimental classification of $\alpha$ decays—instead of a spread of the experimental enhancement coefficients which, as follows from Fig. 3, is more than three orders of magnitude, the ratios $\Gamma^{e}_{L\sigma_f I_f}/\Gamma^{sf}_{L\sigma_f I_f}$ for favored, semifavored, and nonfavored $\alpha$ decays vary only within one order of magnitude, in the range 30–300.

*Binary Correlations in* $^{210}$Pb *and* $^{206}$Pb, *and* $\alpha$ *Decay of* $^{210}$Po. At the first glance it is remarkable, when one examines Fig. 3, that the experimental enhancement coefficients of the Po isotopes are close to those of the Rn, Ra, and Th isotopes, for which the superfluid enhancement coefficients $K_p$ are approximately 10–20. Therefore, to understand the relative variation of the experimental $\alpha$ widths, one must assume that the theoretical proton enhancement coefficients for the Po isotopes containing only two protons in an unfilled shell are of the same order.

Similarly, as can be seen from Fig. 3, the experimental enhancement coefficients for isotones with $N=128$, which contain two neutrons in an unfilled shell, are near those for isotones with $N=130-132$, for which the superfluid coefficients are $K_n=15$. Moreover, the experimental enhancement coefficients for isotones with $N=126$ are near those for isotones with $N=120-124$ ($K_n=10-20$) and do not differ by more than three times from those for isotones with $N=128-132$. In connection with what we have said above, one may expect that for the nonsuperfluid (with respect to the neutron component) isotones $N=126\pm 2$ the correlations in the neutron system are large and lead to theoretical neutron coefficients $K_n=10$.

Since the superfluid model is incorrect in the region of nuclei which have neutron or proton number near that of a magic nucleus, such nuclei are usually treated by the shell model with configuration mixing. The use of the ground-state wave functions of $^{210}$Po and $^{212}$Po obtained by the diagonalization procedure leads to the total enhancement coefficient $K_nK_p=10$ for $^{210}$Po and $K_nK_p=5$ for $^{212}$Po.[33] Such small values of $K_n$ and $K_p$ differ strongly from those required, as pointed out above, to understand the relative variation of the experimental enhancement coefficients. This indicates that in calculations in the shell model with configuration mixing one underestimates the effects of higher configurations, which are of little importance for the description of volume effects (state energy, moments, probabilities of electromagnetic transitions, etc.), but which are important for understanding coherent surface phenomena, which are fundamental in the $\alpha$-decay process.

In this connection, the formalism of two-particle Green's functions[17,34] was used in Ref. 35 to calculate the ground-state wave functions of $^{210}$Po and $^{206}$Pb with allowance for ground-state correlations. These wave functions were used to calculate the theoretical enhancement coefficients for $\alpha$ decay of $^{210}$Po. The one-nucleon shell basis in Ref. 35 was greatly extended by taking into account quasistationary states, and it includes 37 levels for protons and 30 for neutrons, whereas in the diagonalization calculations made earlier only four or five levels in each of the subsystems were used.[36]

As can be seen from Table 5, which shows the neutron and proton theoretical enhancement coefficients, the extension of the shell basis increases $K_n$ and $K_p$ by approximately 2 times and, accordingly, the total enhancement coefficient by 4 times.

The "nonpoint" enhancement coefficients in Table 5 are calculated in the spirit of the hybrid model[22] and give a total enhancement coefficient of order 100. It is interesting to note that allowance for the hole levels for the proton system and the particle levels for the neutron system (ground-state correlations) hardly changes the enhancement coefficients.

The dependence of the proton enhancement coefficient on the number $N_J$ of particle levels used in the diagonalization—the $(2J+1)$-fold degeneracy of each level is taken into account—is shown in Fig. 6. It can be seen that $K_p$ does not tend to saturation when the number of levels taken into account is increased, which corresponds completely to the situation with the theoretical enhancement coefficients in the superfluid model.[25,26] In this connection, allowance for the continuum states can in principle appreciably increase the number of actually combining levels and therefore lead to an additional increase of $K_p$.

Thus, consistent allowance for binary correlations in the case of the $\alpha$ decay of the $^{210}$Po nucleus leads to neutron and proton enhancement coefficients near the corresponding superfluid enhancement coefficients of the neighboring nuclei. This enables one to explain the relative dependence of the experimental enhancement coefficients in the investigated region of nuclei (see Fig. 3). With regard to the theoretical absolute $\alpha$-decay probability of $^{210}$Po, it is, like that for nuclei with developed superfluidity, approximately two orders of magnitude lower than the experimental value.

Summarizing the results of calculations of the $\alpha$ widths of heavy nuclei in the superfluid model and the shell model with configuration mixing, we must point out that although in the framework of these models one can satisfactorily describe the relative $\alpha$ widths, there still remains a discrepancy between the absolute experimental and theoretical $\alpha$-decay probabilities of approximately two orders of magnitude.

*Alpha Decay of Light Nuclei.* Above, we have investigated the $\alpha$ decay of fairly heavy nuclei. However, $\alpha$

TABLE 5.

| System | | Proton | | | | Neutron | | | |
|---|---|---|---|---|---|---|---|---|---|
| Number of levels: | particle | 4 | 4 | 21 | 21 | 5 | 5 | – | 8 |
| | hole | – | 6 | – | 16 | – | 8 | 22 | 22 |
| $K^{pnt}_{p(n)}$ | | 6.5 | 6.78 | 14.47 | 14.83 | 6.23 | 8.25 | 12.1 | 15.92 |
| $K_{p(n)}$ | | 6.78 | 7.19 | 12.34 | 13.03 | 3.8 | 4.5 | 6.16 | 7.42 |

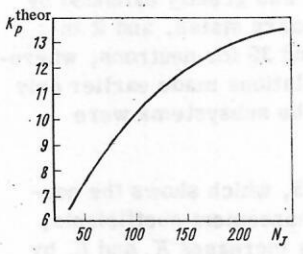


FIG. 6. Theoretical proton enhancement coefficient for $^{210}$Po nucleus as a function of the number $N_J$ of levels taken into account in diagonalization.

radioactivity is also observed in light nuclei, in which, as a rule, $\alpha$ particles are emitted by nuclei from excited states. Until recently, the $\alpha$ widths of light nuclei were analyzed theoretically exclusively on the basis of the $R$ matrix scheme.[37] The reduced widths were calculated at a point $R_0$ in the surface region of the nucleus ($R_0 \approx R_A$), where the concepts of the shell model and, in particular, its oscillator basis are fairly good. At the same time, the $R$-matrix penetration factors were constructed at a different point $R_0'$, which is much further from the center of the nucleus ($R_0' \gtrsim 4$—6 F), no additional matching of the reduced widths and the penetration factors being undertaken. As a result, one has no idea of the accuracy which such a scheme has for the calculation of the absolute $\alpha$-decay probabilities.

In Ref 38, the non-$R$-matrix approach is generalized to the case of $\alpha$ decay of light nuclei of the $1p$ shell, whose wave functions are calculated in Ref. 39 with an oscillator basis in the intermediate-coupling scheme.

To calculate the $\alpha$ widths, the potentials $V_{\alpha A-4}(R)$ are taken to be the potentials given in Refs. 40 and 41, which take into account effectively the experimental data on the elastic scattering of $\alpha$ particles on the daughter nuclei.

The results of the calculations of Ref. 38 for the $\alpha$ decay of the nuclei $^6$Li, $^7$Li, $^7$Be, and $^8$Be are given in Table 6. All the investigated $\alpha$ decays are sub-barrier and satisfy the conditions of applicability of the integral $\alpha$-decay expression (25). As can be seen from Table 6, the experimental and theoretical widths are near for all the investigated nuclei.

Thus, one can hope that the non-$R$-matrix variant of the $\alpha$-decay theory enables one to obtain reasonable agreement with experiment for not only the relative but, more importantly, absolute $\alpha$-decay widths of other light nuclei. The physical reason for this agreement is the approximate equality of the sizes of the $\alpha$ particle and the light nuclei, which means that the wave function of the relative motion of the four nucleons forming the $\alpha$ particle (Young tableau [4]) is near the internal wave function of the $\alpha$ particle even in the case of the shell model without configuration mixing. Because of this, as will be shown below in the case of light nuclei, the corrections to the $\alpha$ widths due to correct allowance for the asymptotic behavior of the $\alpha$-decay channel are unimportant, in contrast to the situation for heavy nuclei.

*Absolute $\alpha$-Decay Probabilities in the Shell Model.* As was pointed out above, the absolute $\alpha$-decay probabilities of heavy nuclei calculated in the shell model are about two orders of magnitude smaller than the experimental values. Let us discuss the extent to which this result is due to the approximations made in the calculations.

First, it is necessary to point out the influence of the phenomenological indeterminacy in the actual choice of the parameters of the shell potentials. As special investigations have shown, the absolute $\alpha$ widths vary on the transition from one type of potential to another only slightly. For example, on the transition from the potential of Ref. 59 ($r_{0p}$ 1.24 F, $r_{0n}$=1.26 F, $a$=0.63 F) to the potential of Ref. 60 ($r_0$=1.28 F, $a$=0.67 F) the $\alpha$ widths increase smoothly by a factor 1.7.

Second, the hybrid scheme used above to calculate the superfluid enhancement coefficients attempts only to reproduce the averaged behavior of the theoretical $\alpha$ widths. Although there are reasons for believing that

TABLE 6.

| Parent nucleus | Excitation energy of daughter nucleus, MeV | $Q_\alpha$, MeV | $I_i^{\pi} i$ | $T_i$ | Spectroscopic factor | Type of decay | $\Gamma_\alpha^{exp}$, keV | $l$ | $R_m$, F | $\Gamma_\alpha^{theor}$, keV | $\Gamma_\alpha^{exp}/\Gamma_\alpha^{theor}$ |
|---|---|---|---|---|---|---|---|---|---|---|---|
| $^6$Li | 2.184 | 0.713 | 3+ | 0 | 1.125 | $\alpha+d$ | 25±1 | 2 | 2.6 | 16.7 | 1.44 |
| | 4.57 | 3.099 | 2+ | 0 | 1.125 | | 350±150 | 2 | 2.55 | 1158 | 0.17 |
| | 6.0 | 4.529 | 1+ | 0 | 1.125 | | 2000 | 2 | 2.55 | 2991 | 0.67 |
| $^7$Li | 4.629 | 2.163 | ≤7/2− | 1/2 | 1.2 | $\alpha+t$ | 93±8 | 3 | 2.75 | 55.4 | 1.54 |
| | 6.56 | 4.094 | 5/2− | 1/2 | 1.2 | | 1000 | 3 | 2.70 | 569.3 | 1.76 |
| | 7.475 | 5.009 | 5/2− | 1/2 | 0.01 | | 36 | 3 | 2.70 | 9.52 | 3.78 |
| $^7$Be | 4.55 | 2.963 | 7/2− | 1/2 | 1.2 | $\alpha+^3$He | 100 | 3 | 2.75 | 94.8 | 1.05 |
| | 6.51 | 4.923 | 5/2− | 1/2 | 1.2 | | 1200 | 3 | 2.77 | 690.3 | 1.74 |
| | 7.185 | 5.598 | 5/2− | 1/2 | 0.01 | | 37 | 3 | 2.77 | 9.2 | 4.0 |
| $^8$Be | 0 | 0.094 | 0+ | 0 | 1.5 | $\alpha+^4$He | (6.8±0.6)·10$^{-3}$ | 0 | 2.95 | 6.9·10$^{-3}$ | 0.9 |
| | 2.9 | 2.994 | 2+ | 0 | 1.5 | | 1450±60 | 2 | 2.95 | 1084 | 1.29 |
| | 11.4 | 11.494 | 4+ | 0 | 1.5 | | 7000 | 4 | 2.8 | 3162 | 2.21 |

the transition to a consistent computational scheme in the framework of the shell model with Woods-Saxon potential would not appreciably change the results, it is very necessary that such calculations be made, despite the serious mathematical difficulties.

Third, there is the possibility of changing the calculated $\alpha$ widths by taking into account higher configurations in the internal wave function of the $\alpha$ particle.[20] Preliminary calculations on the basis of the hybrid model show that the inclusion of such components reduces the theoretical $\alpha$ widths for favored transitions by a factor of order 2.

Finally, there is the question of the influence on the $\alpha$ widths of the neglected second term in the potential $\overline{V}_{\alpha A-4}$ in (26), which is due to the renormalization of the interaction. This interaction evidently has a repulsive nature,[34] which must reduce the theoretical $\alpha$ widths.

Thus, one can conclude that the discrepancy between the experimental and absolute shell $\alpha$ widths obtained above can hardly be eliminated if one stays within the framework of the traditional shell model.

## 3. CLUSTER CONCEPTS IN THE THEORY OF ALPHA DECAY

Above, we have investigated the possibilities of describing the $\alpha$ widths by assuming that the quasistationary wave function of the parent nucleus, $\Psi_{\sigma_i}^{I_i M_i}$, which occurs in Eq. (25), is identical to the shell wave function, $\Psi_{\sigma_i \text{sh}}^{I_i M_i}$, of this nucleus. Note that because the shell basis used in traditional calculations with configuration mixing and the superfluid model is restricted, the wave function $\Psi_{\sigma_i \text{sh}}^{I_i M_i}$ has an asymptotic behavior fundamentally different from the true asymptotic behavior of the quasistationary wave function $\Psi_{\sigma_i}^{I_i M_i}$ (14). In this connection, it is necessary to study the importance of the asymptotic region in the formation of the $\alpha$ width (25) and estimate the order of the errors introduced by the incorrect asymptotic behavior of $\Psi_{\sigma_i \text{sh}}^{I_i M_i}$. Such an investigation can be made on the basis of the notions of $\alpha$ clustering in the surface region of the nucleus.

*Formulation of Cluster Model of Alpha Decay.* It is known that the optical model successfully describes the reaction cross sections and elastic scattering of an $\alpha$ particle on a nucleus by means of a complex optical potential $V_\alpha^{\text{opt}}(R) + iW_\alpha^{\text{opt}}(R)$, which, by its construction, reduces the many-nucleon problem of the interaction of the $\alpha$ particle with the nucleus to the one-particle problem of the motion of the center of mass of the $\alpha$ particle in a potential field. It is assumed that the internal wave function of the $\alpha$ particle is not distorted in the whole region, and the many-particle nature of the problem is approximated by introducing the imaginary correction $W_\alpha^{\text{opt}}(R)$ into the optical potential.

Such an approximation proved fruitful because all the experimental quantities described by the optical model are basically determined by the surface region of the real part of the optical potential.[64] This gives one reason to hope that, at least in the peripheral region of the nucleus, the $\alpha$ particle still preserves its individuality. There are certain additional reasons for such a hope. As follows from Hofstadter's work,[42] for heavy nuclei the density of nucleons at distances $R \geq R_A + 2a$ is reduced by approximately 100 times compared with the density in the center of the nucleus. Therefore, in this region the potential of the interaction between the $\alpha$ particle and the nucleons of the target nucleus can be reasonably calculated using the low-density approximation.[43] In this approximation one can ignore, first, the influence of the Pauli principle, which forbids nucleons of the $\alpha$ particle being in states occupied by nucleons of the target nucleus, and, second, the renormalization of the interaction of the nucleons of the $\alpha$ particle due to the influence of the nucleons of the nucleus [the second term in Eq. (26)]. Then the potential $V_{\alpha A-4}$ (26) can be represented in the simplified form (9). At the same time, the potential $V_{\alpha A-4}$ depends not only on the coordinates of the center of the mass of the $\alpha$ particle, but also on its internal variables. This distorts the internal function of the $\alpha$ particle (polarizability) when it interacts with the target nucleus. As is shown in Ref. 18, in the considered region $R \gtrsim R_A + 2a$ this polarizability can be ignored. Then the optical potential acting on the center of mass of the $\alpha$ particle is[9]

$$V_\alpha^{\text{opt}}(R) = \sum_{i=1}^{4} \int V_i(|\mathbf{R} + \mathbf{r}_i|)\, \rho_\alpha(r_i)\, d\mathbf{r}_i, \tag{40}$$

where $\rho_\alpha(r_i)$ is the distribution density of nucleon $i$ in the $\alpha$ particle.

Thus, these arguments strengthen the hope expressed above that in the surface region of an $\alpha$-decay nucleus the $\alpha$ particle can exist as a cluster separated from the daughter nucleus. This conclusion agrees with the ideas of Ref. 2. Then the wave function of the $\alpha$-decay nucleus in the region $R > R_{c1} = R_A + 2a$ can be represented in the form

$$\Psi_{\sigma_i}^{I_i M_i} = u_{L\sigma_f I_f}^{I_i M_i} \tilde{\Psi}_{L\sigma_f I_f}(R)/R, \tag{41}$$

where $\tilde{\Psi}_{L\sigma_f I_f}(R)$ is the radial function describing the relative motion of the center of mass of the $\alpha$ particle and the daughter nucleus, and in the considered region it coincides with the effective function $\Psi_{L\sigma_f I_f}(R)$ introduced earlier in (33). The function $\tilde{\Psi}_{L\sigma_f I_f}(R)$ has, by virtue of (14), the following asymptotic behavior in the sub-barrier region for $R \leq R_1$:

$$\tilde{\Psi}_{L\sigma_f I_f}(R) \to \sqrt{\Gamma_{L\sigma_f I_f} k/2Q_\alpha}\, G_L(R) \tag{42}$$

and in the region $R_{c1} < R < R_1$ it satisfies the radial Schrödinger equation

$$\left[-\frac{\hbar^2}{2m}\cdot\frac{\partial^2}{\partial R^2} + V_\alpha^{\text{opt}}(R) + \frac{\hbar^2}{2m}\frac{L(L+1)}{R^2} + V_\alpha^{\text{Coul}}(R) - Q_\alpha\right] \times \tilde{\Psi}_{L\sigma_f I_f}(R) = 0. \tag{43}$$

If $\Gamma_{L\sigma_f I_f}$ in the boundary condition (42) is taken to be the experimental $\alpha$ width, then, solving the Schrödinger equation (43), one can continue the real wave function of the quasistationary state $\Psi_{\sigma_i}^{I_i M_i}$ from its far asymptotic behavior (14) into the interior region right down to distances $R \geq R_{c1}$, for which the representation (41) is valid.

Using the function obtained in this way, one can, first, systematically estimate the importance of the asymptotic region in the formation of the $\alpha$ width, and, second, clarify the relationship between the function

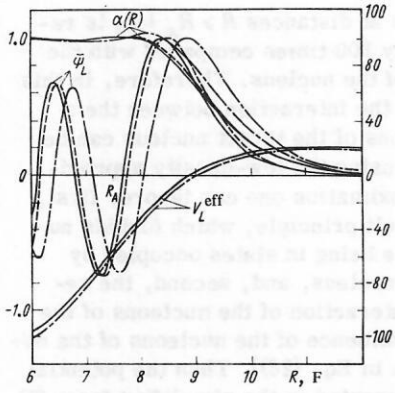


FIG. 7. Dependence of the function $\bar{\Psi}_L(R)$, the potential $V_L^{eff}$, and $\alpha(R)$ on the energy $Q_\alpha$ and the orbital angular momentum $L$: —, - - -, -. -. -. represent the cases $Q_\alpha = 2$ MeV, $L = 5$, $Q_\alpha = 2$ MeV, $L = 0$, and $Q_\alpha = 10$ MeV, $L = 0$, respectively. The functions $\bar{\Psi}_L(R)$ are normalized to unity at the last maximum and the scale for the potential $V_L^{eff}$(MeV) is given on the right.

$\Psi^{I_i M_i}_{\sigma_i \text{sh}}$ used in the shell model and the real quasistationary function and, finally, investigate the possibilities of using the interpolation model[44] to describe $\alpha$ decay.

*Estimate of the Importance of the Asymptotic Region in Forming the Alpha Widths.* Using the integral expression (25) for the $\alpha$ width and the representation (41) of the quasistationary wave function $\Psi^{I_i M_i}_{\sigma_i}$, we introduce

$$\Gamma_{L\sigma_f I_f}(R) = 2\pi \left| \int_R^{R_1} \bar{\Psi}_{L\sigma_f I_f}(R') V_\alpha^{\text{opt}}(R') \bar{F}_L(R') R' dR' \right|^2, \quad (44)$$

which determines the contribution to the $\alpha$ width of the asymptotic region from $R$ to $R_1$, where $R \geq R_{\text{cl}}$. It is convenient to introduce the dimensionless ratio

$$\alpha^2(R) = \Gamma_{L\sigma_f I_f}(R)/\Gamma_{L\sigma_f I_f}, \quad (45)$$

which gives the relative contribution of this region to the $\alpha$ width. Then, introducing the function

$$\bar{\Psi}_L(R) = (\Gamma_{L\sigma_f I_f} k/2Q_\alpha)^{-1/2} \bar{\Psi}_{L\sigma_f I_f}(R), \quad (46)$$

which satisfies the Schrödinger equation (43), and which, by (42), has the asymptotic behavior

$$\bar{\Psi}_L(R) \to G_L(R), \quad (46')$$

we obtain, using the relationship (18) between the function $\bar{F}_L(R)$ and the regular Coulomb function $F_L(R)$, the following expression for $\alpha^2(R)$:

$$\alpha^2(R) = \frac{k^2}{Q_\alpha^2} \left| \int_R^{R_1} \bar{\Psi}_L(R') V_\alpha^{\text{opt}}(R') F_L(R') dR' \right|^2. \quad (47)$$

It is interesting to note that the function $\alpha^2(R)$ defined by Eq. (47) does not depend on the $\alpha$ width $\Gamma_{L\sigma_f I_f}$ but is completely determined by the kinematics of the $\alpha$ decay and the potential $V_\alpha^{\text{opt}}(R)$.

For the $^{210}$Bi nucleus, we show in Fig. 7 the functions $\bar{\Psi}_L(R)$, normalized for greater lucidity to unity at the last maximum, the potentials $V_L^{\text{eff}}(R)$, which are equal to the sum of the nuclear, Coulomb, and centrifugal potentials, and also the functions $\alpha(R)$ for different values of $L$ and $Q_\alpha$. All the quantities in Fig. 7 were obtained with the potential $V_\alpha^{\text{opt}}(R)$ from Ref. 9.

As detailed calculations showed, the behavior of the functions $\bar{\Psi}_L(R)$ and $\alpha(R)$, referred to the position of the radius $R_A$ of the nucleus, depends weakly on the mass number $A$, the charge $Z$, the energy $Q_\alpha$, and the angular momentum $L$ (for $L \leq 8$). The results given in Fig. 7 are typical of the whole region of heavy spherical nuclei considered above.

As can be seen from Fig. 7, the position of the maximum of the function $\bar{\Psi}_L(R)$ is almost independent of $L$ and is shifted by not more than 0.4 F when the energy is changed from 2 to 10 MeV, which covers the range of variation of the experimental $Q_\alpha$. The situation as regards the $L$ dependence changes for $L > 8$, when a sharp increase of the centrifugal barrier appreciably shifts the maximum of the function $\bar{\Psi}_L(R)$ into the interior region.

An important result which follows from Fig. 7 is that $\alpha(R_{\text{cl}}) \geq 0.9$, this being true for all the investigated cases with $L \leq 8$. Thus, the main contribution to the $\alpha$ width accumulates in the peripheral region, in which one can reckon on the applicability of the cluster model. This means that in any theoretical approach which ignores the cluster asymptotic behavior one can hardly hope to obtain correct absolute $\alpha$-decay probabilities of heavy nuclei.

*Limiting Cluster Model.* Above, the idea of $\alpha$ clustering has been used in the regions in which it is more or less justified.

Below, we consider the limiting cluster model of $\alpha$ decay, in which it is assumed that the division into a daughter nucleus and an $\alpha$ particle, between which the nonpolarizing potential $V^{\text{opt}}_{\alpha A-4}(R)$ acts, is valid in the whole region. A "one-particle" model of this kind was considered earlier in Ref. 46, in which the potential $V^{\text{opt}}_{\alpha A-4}(R)$ was chosen in such a way that the positions of the resonances for scattering on this potential coincide with the experimental $\alpha$-decay energies. Then, investigating the elastic-scattering cross section with a small energy step $\delta_E$ in the neighborhood of $Q_\alpha$, Scherk and Vogt[46] obtained the widths $\Gamma_\alpha^{\text{cl}}$ of these quasistationary states. Although such a procedure can give an exact result, it is complicated in application, requiring a large number of calculations with high accuracy ($\delta_E < \Gamma_\alpha^{\text{cl}}$). It was evidently for this reason that Scherk and Vogt restricted themselves to the case of the $^{212}$Po nucleus, for which the $\alpha$ width has one of the largest values, approximately equal to $10^{-15}$ MeV.

Applying the formalism set forth above, the problem of calculating the widths $\Gamma_\alpha^{\text{cl}}$ can be solved much more simply than in Ref. 46, and this therefore makes the cluster model a convenient tool for analyzing experimental $\alpha$ decays. In the "one-particle" cluster model, the function $\bar{\Psi}_{L\sigma_f I_f}(R) \equiv \Psi_L(R)$ coincides by definition with the effective function $\Psi_{L\sigma_f I_f}(R)$ and satisfies the Schrödinger equation (43) in the whole region $0 \leq R \leq R_1$. Integrating Eq. (43) for the function $\bar{\Psi}_L(R)$ from the point $R_1$ inside the nucleus with the boundary condition

(42) and choosing the parameters of the potential $V^{\text{opt}}_{\alpha A-4}(R)$ in such a way that

$$\bar{\Psi}_L(0)=0, \tag{48}$$

we obtain a function $\bar{\Psi}_L(R)$ which differs from the normalized function $\Psi_L(R)$ only by the constant factor

$$\Lambda=\left[\int_0^{R_1}\bar{\Psi}^2_L(R)\,dR\right]^{-1/2}. \tag{49}$$

As we have shown above, under sub-barrier conditions the function $\Psi_L(R)$ in the interval $0\leqslant R\leqslant R_1$ has the same form as the one-particle resonance scattering function and is related to it by Eq. (21).

Now, using the integral expression (34), we can readily calculate the cluster one-particle $\alpha$ width. However, in this case the $\alpha$ width can be obtained by a more elegant method. Using the definition (46), we write

$$\Gamma^{\text{cl}}_L=\frac{2kR}{\bar{\Psi}^2_L(R)}\left[\frac{\hbar^2}{2mR}\Psi^2_L(R)\right]\equiv 2P^{\text{cl}}_L(R)\,\gamma^2_{L\,\text{cl}}(R). \tag{50}$$

The expression (50) for the $\alpha$ width has the usual $R$-matrix form[4,46] factorized into the penetratability $P^{\text{cl}}_L(R)$ and the reduced cluster width $\gamma^2_{L,\text{cl}}(R)$. However, in contrast to the standard approach,[46] one can make a further important step by noting that, because of the special choice of $V^{\text{opt}}_{\alpha A-4}(R)$, which ensures fulfillment of the condition (48), the right-hand side in Eq. (50) holds for all values of $R$, so that, taking into account Eq. (49), we obtain

$$\Gamma^{\text{cl}}_L=2Q_\alpha\Lambda^2/k. \tag{51}$$

Thus, we have solved the problem of calculating the cluster widths of sub-barrier $\alpha$ decay without using the integral expression (34). Note that Eq. (51) was first obtained by Breit,[65] though it was not used in subsequent investigations.

We shall compare the experimental and theoretical $\alpha$ widths by means of the experimental cluster enhancement coefficients:

$$K^{\text{cl}}_e=\Gamma^e_\alpha/\Gamma^{\text{cl}}_L, \tag{52}$$

which are equal to the spectroscopic factors $S^{\eta L}_{\lambda c}$ introduced in Ref. 46. In addition, the experimental cluster enhancement coefficients are exact analogs of the dimensionless reduced widths expressed in units of the Wigner limit.[5] However, the coefficients $K^{\text{cl}}_e$ are calculated for a realistic well with smooth edge and do not depend on the channel radius.

Note that earlier, using the penetration factor $P^{\text{cl}}_L(R_0)=kR_0/\bar{\Psi}^2_L(R_0)$, the experimental reduced widths for the $\alpha$ decay of compound states were calculated for a number of intermediate and heavy nuclei[47,48] and also for the doubly even isotopes[49] of Po. Since the channel radius $R_0$ in these calculations was taken near the last maximum of the function $\bar{\Psi}_L(R)$, and the reduced cluster width $\gamma^2_{L,\text{cl}}(R_0)$ introduced in Eq. (50) is virtually constant for all sufficiently heavy nuclei, the ratio between the values obtained for the experimental reduced widths and the corresponding values of $K^{\text{cl}}_e$ must reduce to a constant.

*Probabilities for the Existence of an Alpha Particle in the Surface Region of the Nucleus, and Classification of Alpha Decays.* Using, as we have shown above, the experimental $\alpha$ width in conjunction with Eq. (43) and the boundary condition (42), we can obtain the "experimental" cluster function $\tilde{\Psi}_{L\sigma_f I_f}(R)$ in the region $R_1\geqslant R\geqslant R_{\text{cl}}$. Using this function, we estimate the probability $W^{L\sigma_f I_f}_\alpha$ of finding an $\alpha$ particle in the clustering region ($R\geqslant R_{\text{cl}}$):

$$W^{L\sigma_f I_f}_\alpha=\int_{R_{\text{cl}}}^{R_1}\tilde{\Psi}^2_{L\sigma_f I_f}(R)\,dR. \tag{53}$$

Using the universality of the radial behavior of the function $\tilde{\Psi}_{L\sigma_f I_f}(R)$, we integrate in Eq. (53) and write the probability $W^{L\sigma_f I_f}_\alpha$ in terms of the value of this function at the maximum, $\tilde{\Psi}_{L\sigma_f I_f}(R_m)$, by means of the approximate relation

$$W^{L\sigma_f I_f}_\alpha\approx 0.75\tilde{\Psi}^2_{L\sigma_f I_f}(R_m). \tag{54}$$

Then, expressing the experimental $\alpha$ width by means of (46) in terms of $\tilde{\Psi}_{L\sigma_f I_f}(R)$ and using Eq. (50), we obtain $K^{\text{cl}}_e$ in the form

$$K^{\text{cl}}_e=\tilde{\Psi}^2_{L\sigma_f I_f}(R_m)/\Psi^2_L(R_m). \tag{55}$$

Since $\Psi_L(R_m)\approx 0.6\ \text{F}^{-1/2}$ for all the investigated cases, Eq. (54) can be used to relate the probability of finding an $\alpha$ particle in the clustering region to the coefficient $K^{\text{cl}}_e$ by means of the equation

$$W^{L\sigma_f I_f}_\alpha=0.27K^{\text{cl}}_e. \tag{56}$$

The classification of $\alpha$ decays with respect to the experimental cluster enhancement coefficients or the experimental reduced widths (subject to the condition $R_0=R_m$) is mathematically equivalent to the classification with respect to the probabilities $W^{L\sigma_f I_f}_\alpha$, though the latter is physically more consistent since the treatment of $\alpha$ decay in terms of $W^{L\sigma_f I_f}_\alpha$ is close in spirit to the ideas of surface $\alpha$ clustering[44] and does not require the assumption that the $\alpha$ particle exists in the interior region of the nucleus.

Figure 8 shows $W^{L\sigma_f I_f}_\alpha$ calculated with the potential $V^{\text{opt}}_{\alpha A-4}(R)$ of Ref. 9 for the investigated $\alpha$ decays. In Fig. 8 one can see a tendency for the $\alpha$ decays to be divided

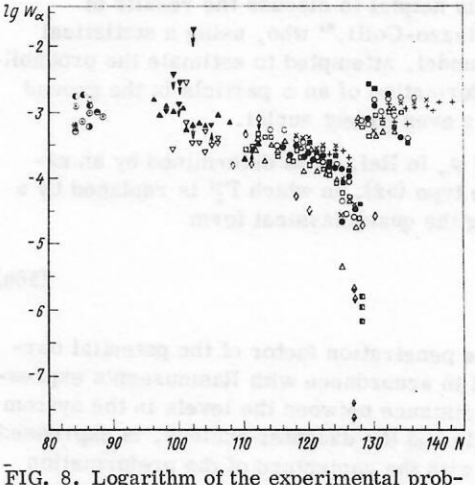


FIG. 8. Logarithm of the experimental probability $W^{L\sigma_f I_f}_\alpha$ of finding an $\alpha$ particle in the surface region of the nucleus as a function of the neutron number $N$. The elements are denoted as in Fig. 3.

into groups in accordance with the degree of "$\alpha$-one-particle forbiddenness", which corresponds completely to the classification of $\alpha$ decays in the shell model in accordance with the degree of favoredness (see Fig. 3). Since Figs. 3 and 8 have much in common, we can, without repeating what we said earlier in connection with Fig. 3, point out just three important points.

The first is that the classification of $\alpha$ decays in accordance with $W_\alpha^{L\sigma_f I_f}$ has as much predictive power as the shell classification. The values of $T_{1/2}^\alpha$ predicted by means of the cluster model for a number of unreliably measured $\alpha$ decays agree well with the predictions based on the shell model and given in Table 3.

The second is that the behavior of $W_\alpha^{L\sigma_f I_f}$ is correlated to the dependence of the theoretical enhancement coefficients (see Fig. 5). This is a phenomenological indication that the probability of existence of an $\alpha$ particle in the surface region $R \geqslant R_{cl}$ is simulated by the amplitude of the function $\Psi_{L\sigma_f I_f}^{sh}(R)$ calculated in the framework of the shell model with allowance for pairing correlations.

The third is that the values of $W_\alpha^{L\sigma_f I_f}$ are significantly smaller than unity and equal on the average to $7 \cdot 10^{-4}$, $3 \cdot 10^{-5}$, and $8 \cdot 10^{-7}$ for favored, semifavored, and unfavored $\alpha$ decays, respectively.

Note that the values of $W_\alpha^{L\sigma_f I_f}$ were obtained using the theoretical potential of Ref. 9 for $V_{\alpha A-4}^{opt}(R)$. The transition to the phenomenological potentials of Ref. 50 increases the probabilities $W_\alpha^{L\sigma_f I_f}$ by approximately constant factors—about three for the sets $b$ and $c$ and about six for the set $a$. These changes in the values of $W_\alpha^{L\sigma_f I_f}$ are due to the reduction of the penetration factor resulting from the increased width of the potential barrier. Since all phenomenological potentials must be close to one another in the region of the barrier, the conclusion that the probabilities $W_\alpha^{L\sigma_f I_f}$ are small is universal. This, in its turn, means that if the cluster levels do exist[44] they are weakly coupled to the ground states of the nuclei.

In the light of the deduced smallness of the probabilities $W_\alpha^{L\sigma_f I_f}$, it is helpful to discuss the results of Bonetti and Milazzo-Colli,[61] who, using a statistical preformation model, attempted to estimate the probability $\varphi_\alpha$ for the formation of an $\alpha$ particle in the ground states of doubly even parent nuclei.

The value of $\varphi_\alpha$ in Ref. 61 is determined by an expression of the type (52), in which $\Gamma_L^{cl}$ is replaced by a width $\Gamma_0$ having the quasiclassical form

$$\Gamma_0 = \frac{D_\alpha}{2\pi} \overline{P}_L, \tag{56a}$$

where $\overline{P}_L$ is the penetration factor of the potential barrier calculated in accordance with Rasmussen's expression[1]; $D_\alpha$, the distance between the levels in the system of the $\alpha$ particle and the daughter nucleus, is expressed in accordance with the conjecture of the preformation model in terms of the density $g_{sh}$ of shell states near the Fermi level by the equation

$$D_\alpha = 4/g_{sh} \approx (0.25 - 1)\ \text{MeV}^{-1}. \tag{56b}$$

The values of $\varphi_\alpha$ obtained in Ref. 61 for favored transitions are $\varphi_\alpha = 0.7-0.01$, which is approximately 20—50 times greater than the corresponding values of the experimental cluster enhancement coefficients calculated for the potential $V_{\alpha A-4}$ used in Ref. 61.

Note that the cluster width $\Gamma_L^{cl}$ in the quasiclassical approximation can also be represented in the form (56a), and that $D_\alpha^{cl} \approx 20$ MeV is close to the distance between the resonance states with given $L$ for scattering in the potential $V_{\alpha A-4}^{opt}$. Then the difference noted above between the experimental cluster enhancement coefficients and $\varphi_\alpha$ can be entirely explained by the difference between $D_\alpha^{cl}$ and $D_\alpha$. Since the estimate of the probability for the formation of an $\alpha$ particle in the parent nucleus by means of the experimental cluster enhancement coefficients is close to the value of $W_\alpha^{L\sigma_f I_f}$, which does not require the assumption of volume clustering, one can conclude that the densities $D_\alpha$ of the $\alpha$-particle levels [Eq. (56b)] used in Ref. 61 are unreasonably overestimated.

*Alpha Decay of Compound States.* In recent years $(n,\alpha)$ reactions have been used[51] to obtain data on the $\alpha$-decay widths of highly excited states for a number of intermediate and heavy nuclei ($64 \leqslant A \leqslant 178$). In some cases, only the total $\alpha$ widths are known,[52] but sometimes[53,54] one can measure directly the partial $\alpha$ widths $\Gamma_{L\sigma_f I_f}$. From an analysis of the two-step reaction $^{143}\text{Nd}(n,\gamma\alpha)^{140}\text{Ce}$ (see Ref. 55) one can obtain information about the $\alpha$ widths of compound states lying below the threshold for neutron emission. In the general picture of $\alpha$ decay, these data occupy a distinguished position because of the exceptional complexity of the wave functions of the original states of the parent nuclei. For the semimicroscopic description of these states being currently developed,[56] it is very important to extract from the experimental neutron and $\gamma$ widths averaged values for the different components of the wave functions of the compound states. In turn, an analysis of the $\alpha$ widths of these states can give information about the wave-function components which are not important for decay with the emission of neutrons and $\gamma$ rays.

The use of the shell model to analyze the experimental $\alpha$ widths of highly excited states encounters fundamental difficulties.

First, because of the high excitation energy there is a very great increase in the number of shell states which can contribute significantly to the wave function of the $\alpha$-decay nucleus, and this renders any microscopic calculations extremely tedious and strongly dependent on the choice of the particular diagonalization model.

Second, one can question the applicability of the diagonal (with respect to the core) approximation used in calculations of the shell $\alpha$ widths. Therefore, in what follows we analyze the $\alpha$ decay of neutron resonances on the basis of the cluster model.

The treatment will be given in terms of the enhancement coefficients $K_\alpha^{cl}$, which are a measure of the volume $\alpha$ clustering. If it is remembered that the probabilities $W_\alpha$, which are a measure of the surface $\alpha$ clustering, differ from the values of $K_\alpha^{cl}$ only by a factor approximately equal to 4 and that the indeterminacy in

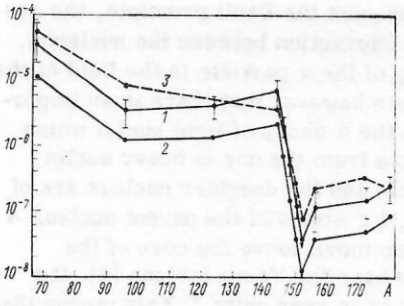


FIG. 9. Comparison of the ratios $\overline{\Gamma}_\alpha^c/\Gamma_\alpha^{cl}$ (curves 1 and 2) and $\overline{D}_c/D_{0,cl}$ (3) for $\alpha$ decay of the compound states of nuclei with mass number $A$.

the choice of the optical potentials gives a comparable spread in the values of $K_e^{cl}$ and $W_\alpha$, one can hardly choose between the volume and surface $\alpha$-clustering models on the basis of the existing data for the compound-state $\alpha$ widths.

Since the $\alpha$ widths of individual compound states fluctuate strongly, satisfying the Porter-Thomas distribution,[53] we shall use for the following analysis the $\alpha$ widths averaged over all measured resonances. Thus, the information we obtain is by definition statistical in nature.

In the following treatment we use the approach proposed in Ref. 57. It is well known that the existing experimental data on the averaged neutron and $\gamma$ widths (for hard transitions with $E_\gamma$ of the order of the neutron binding energy) of compound resonances can be described satisfactorily by the equation

$$\overline{\Gamma}_c = \Gamma_0 \overline{D}_c / D_0. \tag{57}$$

Here, $\Gamma_0$ is the corresponding width in the one-particle model; $\overline{D}_c$ is the average distance between the compound levels; $D_0 \approx 15$ MeV is the interval between one-particle states with given $I_i^{\pi i}$. Thus, the one-particle enhancement coefficients for neutron and $\gamma$ decays of the compound states is $\overline{D}_c/D_0$.

In Fig. 9, we compare the experimental cluster enhancement coefficients for the $\alpha$ decay of the compound states of a number of intermediate and heavy nuclei (points joined by continuous lines) with the values of the ratio $\overline{D}_c/D_{cl}$ (dashed line), where $D_{cl} \approx 23$ MeV is the distance between the cluster levels in the potential $V_{\alpha A-4}^{opt}(R)$. The values of the experimental cluster enhancement coefficients (curve 1) were taken for the potential $V_{\alpha A-4}^{opt}$ from Ref. 9, and the points of curve 2 were calculated with the potential $c$ of Ref. 50. For curve 1, we have plotted the experimental errors in the determination of the average $\alpha$ widths, which are due primarily to the sparse statistics of the averaging (see Ref. 58 for details). It can be seen from the figure that, to within the uncertainty connected with the choice of the type of potential $V_{\alpha A-4}^{opt}$, Eq. (57) is also valid for the $\alpha$ widths of neutron resonances.[1)] From this some important conclusions follow.

First, the cluster model has a classifying and, therefore, predictive power for the $\alpha$ decay of compound states as well.

Second, from the point of view of the shell model it is hard to understand Eq. (57) when applied to $\alpha$ widths; for consider $\alpha$ decays from compound states with $I_i^{\pi i} \neq 0^+$ to ground states of daughter nuclei with $I_f^{\pi f} = 0^+$. In this case, an $\alpha$ decay of semifavored type could be predominant from the point of view of the shell model. One would imagine that the weight of the corresponding shell state in the compound wave function is in order of magnitude equal to the ratio $\overline{D}_c/D_2$, where $D_2 \approx 1$ MeV is the average distance between two-quasiparticle levels with $I^\pi = I_i^{\pi i}$. Then, since $K_e^{cl} \approx 10^{-4}$ for semifavored $\alpha$ decays, one can obtain the following estimate for the $\alpha$ width of the compound states:

$$\overline{\Gamma}_c^\alpha = K_e^{cl} \Gamma_{cl} \frac{\overline{D}_c}{D_2} = \Gamma_{cl} \frac{\overline{D}_c}{D_{cl}} \cdot 10^{-3}. \tag{58}$$

A similar estimate for $\overline{\Gamma}_c^\alpha$ can also be obtained in the case of an unfavored (four-quasiparticle) mechanism of compound-state $\alpha$ decay. Thus, the shell estimate of $\overline{\Gamma}_c^\alpha$ in (58) is appreciably lower than the experimental value of the average $\alpha$ width even if one discounts the inaccuracy in the knowledge of the distance between the two- and four-quasiparticle levels with given $I_i^{\pi i}$. One gets the impression that Eq. (57) must be interpreted as an experimental indication of a cluster nature of the wave-function components of the compound state that are responsible for the $\alpha$ decay.

Third, noting that the $\alpha$-particle force function defined by $(\overline{\gamma}_{\alpha c}^2)_{exp}/\overline{D}_c \sim K_e^{cl}/D_c$ is virtually independent of the mass number for the investigated region of nuclei (see Fig. 9), it is reasonable to conclude that the spread of the cluster components over the compound states is large.

Note finally that the above results apparently indicate a change of the $\alpha$-decay mechanism with increasing excitation energy of the parent nucleus.

*Relation between Cluster Model and Shell Model.* Because $\alpha$ decay from highly excited states of nuclei is so complicated, we shall restrict ourselves below to investigating $\alpha$ decay from low-lying or ground states.

We consider first the case of heavy parent nuclei. If, following Ref. 44, we assume that in the description of the $\alpha$-decay process the assumptions of the shell model are valid in the range $R \leq R_{sh} \approx R_A$, then the effective wave function $\Psi_{L\sigma_f I_f}(R)$ in (33) must coincide in this region with the function $\Psi_{L\sigma_f I_f}^{sh}$ introduced above.

On the other hand, as we have already pointed out, the wave function $\Psi_{L\sigma_f I_f}(R)$ will coincide with the "experimental" cluster function $\tilde{\Psi}_{L\sigma_f I_f}(R)$ for values $R > R_{cl}$. Thus, the function $\tilde{\Psi}_{L\sigma_f I_f}(R)$ is a continuation of the function $\Psi_{L\sigma_f I_f}^{sh}(R)$ into the exterior region. Figure 10 compares the shell superfluid function $\Psi_{L\sigma_f I_f}^{sh.sf}(R)$ and the cluster function $\tilde{\Psi}_{L\sigma_f I_f}(R)$ for the case of the $^{216}$Ra nucleus with developed superfluidity. As can be seen from Fig. 10, the amplitude of the function $\tilde{\Psi}_{L\sigma_f I_f}(R)$ at the maximum is 3 times greater than the amplitude of

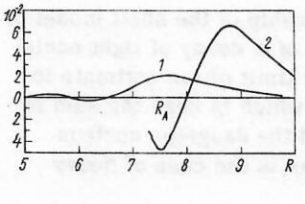


FIG. 10. Comparison of the shell superfluid effective function $\Psi_{L\sigma_f I_f}^{sh.sf}(R)$ (1) with the cluster effective function $\tilde{\Psi}_{L\sigma_f I_f}(R)$ (2) for the $\alpha$ decay of $^{216}$Ra; $R_A$ is the range of the shell potential.

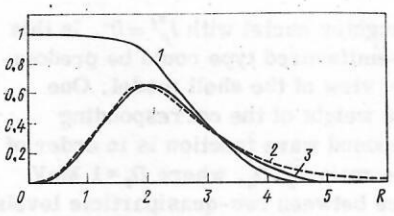


FIG. 11. Comparison of the shell effective function (3) with the cluster function $\tilde{\Psi}_{L\sigma_f I_f}(R)$ (2) for the $\alpha$ decay of $^6$Li. Curve 1 is the function $\alpha(R)$.

the last ($R \approx R_A$) maximum of $\Psi^{\text{sh-sf}}_{L\sigma_f I_f}(R)$. Figure 10 gives fairly typical results, since because of the large number of shell configurations forming the function $\Psi^{\text{sh-sf}}_{L\sigma_f I_f}(R)$ its form for all favored $\alpha$ transitions is as universal as that of the function $\tilde{\Psi}_{L\sigma_f I_f}(R)$. The ratio of the amplitudes of these functions can vary from 0.4 to 3.2 within the group of favored $\alpha$ decays. In the case of semifavored and unfavored $\alpha$ decays (with $L \leq 8$) the above ratio of the amplitudes remains approximately the same as for a favored $\alpha$ decay.

For the following treatment, it is convenient to modify the expression (34) for the $\alpha$ width. Since, as numerical calculations show, the potential $V^{\text{opt}}_{\alpha}(R)$ in (40) differs only slightly from the potential $V_{\alpha A-4}(R)$ in (31) in the region $R \leq R_A + a$ [$a$ is the diffuseness of the potential (10)], Eq. (34) for the $\alpha$ width can be written in the form

$$\Gamma_{L\sigma_f I_f} = 2\pi \left| \int_0^{R_1} \Psi_{L\sigma_f I_f}(R)\, V^{\text{opt}}_{\alpha}(R)\, \tilde{F}^{\text{in}}_{\alpha}(R)\, R\, dR \right|^2. \qquad (59)$$

If, further, we split the domain of integration in (59) into the two intervals $0 \leq R \leq R_{\text{cl}}$ and $R_{\text{cl}} \leq R \leq R_1$, then, as is well known, the first interval, which basically determines the absolute $\alpha$ width in the shell model, makes a contribution of the order of or less than 1% to the total width (59), whereas the contribution of the second interval, in which the assumptions of $\alpha$ clustering are valid, is predominant.

The above splitting is a very crude approximation, which ignores the importance of knowing the details of the transition from the function $\Psi^{\text{sh}}_{L\sigma_f I_f}$ to the function $\tilde{\Psi}_{L\sigma_f I_f}$, this transition being determined basically by the many-particle character of the $\alpha$-decay process. Nevertheless, since the decisive role of the peripheral regions in forming the absolute $\alpha$ widths has been established on the basis of the asymptotic behavior of the quasistationary function $\Psi^{I_i M_i}_{\sigma_i}$ and without appealing to the experimental $\alpha$ widths, it is clear that only by combining the shell model of $\alpha$ decay, which takes into account the structure of the decaying nucleus, and the cluster model, which contains the correct asymptotic behavior of the $\alpha$ decay, can one hope to explain the relative and absolute $\alpha$ widths for heavy nuclei.

Let us consider the relationship of the shell model to the cluster model in the case of $\alpha$ decay of light nuclei of the $1p$ shell.[38] As an upper limit of the estimate for $R_{\text{cl}}$ one can take $R_{\text{cl}} = 3.5$ F, which is near the sum of the radii of the $\alpha$ particle and the daughter nucleus. For $R < R_{\text{cl}}$ it is necessary, as in the case of heavy nuclei, to take into account the Pauli principle, the renormalization of the interaction between the nucleons, and the polarizability of the $\alpha$ particle in the field of the daughter nucleus. Note however that there is an important circumstance in the $\alpha$ decay of light nuclei which distinguishes this case from the one in heavy nuclei. Because the $\alpha$ particle and the daughter nucleus are of about the same size, for states of the parent nucleus $A$ in which four nucleons move above the core of the daughter nucleus and have the Young tableau [4], the spectroscopic factor $s^{\alpha}$ is near unity.[37] This means that for such states the $\alpha$ particle can exist as a whole with a high probability within the parent nucleus, despite the influence of the factors mentioned above.

Such shell states should appear as resonances in the channel of $\alpha$-particle elastic scattering on the daughter nucleus with corresponding quantum numbers and energies near those of these shell states. These resonances can be described directly in the language of the wave function of the motion of the center of mass of the $\alpha$ particle with respect to the daughter nucleus by means of the optical potentials introduced in Refs. 40 and 41. Note that the $\alpha$ particle can also exist as a whole within the parent nucleus with amplitude $\sqrt{s^{\alpha}}$ for all $\alpha$ decays in which the diagonal approximation is valid. But then for such states $R_{\text{cl}}$ and the relationship between the cluster function $\tilde{\Psi}_{L\sigma_f I_f}(R)$ and the effective function $\Psi_{L\sigma_f I_f}(R)$ become quite different from the case of heavy nuclei. As can be seen from Fig. 11, which gives the results for the $\alpha$ decay of an excited state of $^6$Li($E_{\text{exc}} = 2.184$ MeV, $I^{\pi}_i = 3^+$, $Q_{\alpha} = 0.71$ MeV, $L = 2$) the value of $\alpha(R)$ (curve 1) calculated on the basis of the potential $V^{\text{opt}}_{\alpha A-4}$ of Ref. 40 reaches the value 0.9 only for a point $R \approx 1$ F, which lies in the interior region of the parent nucleus. At the same time, the functions $\Psi_L(R)$ and $\Psi^{\text{sh}}_{L\sigma_f I_f}(R)$ (curves 2 and 3, respectively) are close in the interior region and differ only in the asymptotic region ($R \gtrsim 3.5$ F), whose contribution to the $\alpha$ width is not more than 5% [$\alpha(3.5) \approx 0.2$].

Thus, in the case of light nuclei the asymptotic region, in which the shell wave function $\Psi^{\text{sh}}_{L\sigma_f I_f}$ differs strongly from the function $\tilde{\Psi}_{L\sigma_f I_f}$ (which gives the correct $\alpha$-decay asymptotic behavior), makes a small contribution to the $\alpha$ widths. This explains why the absolute $\alpha$ widths calculated above on the basis of the shell model (see Table 6) agree well with the experimental values.

Thus, analysis of the situation in the shell model and cluster model of $\alpha$ decay shows that one must learn how to fit the cluster function $\tilde{\Psi}_{L\sigma_f I_f}$ to the effective function $\Psi^{\text{sh}}_{L\sigma_f I_f}$. This is a very difficult problem but we hope that it can be solved by a more realistic choice of the effective interactions and allowance for continuum states in the diagonalization.

## CONCLUSIONS

The theory of knowledge teaches that the only theoretical schemes which survive are those capable of predicting new facts on the basis of a more penetrating analysis of existing facts. But it is precisely for such theories that experiments can give important indications concerning the validity of the basic assumptions and point out the correct direction of further development.

We should therefore like to draw the attention of experimenters to a number of problems which are important for progress in understanding $\alpha$ decay. In order to clarify the possibilities of the shell model (with allowance for nucleon-nucleon correlations) for quantitative description of the experimental classification of $\alpha$ decays, it is necessary to extend greatly the data on semifavored and unfavored $\alpha$ decays, including at the least information on the spins and parities of the states of the parent and daughter nuclei.

Such a request does not diminish interest in the traditional investigations of new spontaneously $\alpha$-radioactive nuclei, for which $\alpha$ decay is in many cases the only process capable of giving information about their structure.

At the present time there are virtually no known cases (except perhaps for the $^{218}$Ac nucleus and also the isotopes $^{178}$Au, $^{179}$Au, and $^{181}$Au, for which there are only upper limits for the $\alpha$ widths) for which the experimental enhancement coefficients $K_e = \Gamma_\alpha^e / \Gamma_\alpha^{sh}$ appreciably exceed the average values of the experimental enhancement coefficients for favored $\alpha$ decays of nuclei with neighboring neutron numbers.

However, experimental searches for such cases and repeated measurements of the existing deviations are important for our understanding of the role played by $\alpha$ clustering in the ground states of $\alpha$-decay nuclei.

Further, in the light of the indications of a possible change of the $\alpha$-decay mechanism with increasing excitation energy of the parent nucleus, particular interest attaches to a further study of the averaged and individual partial $\alpha$ widths for as many highly excited states (and nuclei) as possible by means of $(n,\alpha)$ and $(p,\alpha)$ reactions. In this connection, analysis of the energy spectra of the $\alpha$ particles would be particularly helpful. We should like to point out the attraction of $(^6\mathrm{Li}, d)$ and $(^7\mathrm{Li}, t)$ $\alpha$-particle transfer reactions as means for obtaining information about the reduced $\alpha$ widths of ground and highly excited states of nuclei that do not exhibit spontaneous $\alpha$ radioactivity.

Note finally that in this review we have not discussed at all the large region of deformed nuclei in which there are possibilities for studying the influence of nuclear structure on the $\alpha$-decay probability. This was done deliberately. Although a non-$R$-matrix approach has been formulated[62] for the $\alpha$ decay of deformed nuclei, it has not yet been used systematically to analyze experimental data.

We should like to express our gratitude to V.E. Kalechits, A.A. Martynov, Yu.V. Ratis, K.S. Rybak, G. Stratan, S. Kholan, Yu.I. Kharitonov, and V.G. Khlebostroev, who collaborated with us in obtaining some of the results given here. We should also like to thank A.I. Baz', Yu.P. Popov, V.G. Solov'ev, and L.A. Sliv for helpful discussions of a number of problems connected with $\alpha$ decay.

[1)]Equation (57) does not contradict the conclusion of Ref. 48 that the experimental reduced neutron widths of compound states are greater than the corresponding reduced $\alpha$ widths; for it follows from (50) and (57) that the averaged reduced widths must satisfy $[\gamma_n^2(R_m)/\gamma_{\alpha cl}^2(R_m)] = 8$.

[1]J.O. Rasmussen Phys. Rev. **113**, 1593 (1959).
[2]A.I. Baz', in: Materialy VI Zimneĭ Shkoly po Teorii Yadra i Fiziki Vysokikh Energiĭ (Proc. Sixth Winter School on Nuclear Theory and High-Energy Physics), Part I, Nauka, Leningrad (1971).
[3]R.G. Thomas, Prog. Theor. Phys. **12**, 253 (1954).
[4]H.J. Mang, Z. Phys. **148**, 582 (1957); H.J. Mang, Phys. Rev. **119**, 1069 (1960).
[5]A.M. Lane and R.G. Thomas, "$R$-matrix theory of nuclear reactions," Rev. Mod. Phys. **30**, 257 (1958).
[6]D.H. Wilkinson, in: Modern Problems of Nuclear Physics [Russian translation from the English], Gosatomizdat, Moscow (1963).
[7]K. Harada and E.A. Rauscher, Phys. Rev. **169**, 818 (1968).
[8]H. Feshbach, Ann. Phys. **5**, 357 (1958).
[9]S.G. Kadmenskiĭ *et al.*, Yad. Fiz. **10**, 730 (1970) [Sov. J. Nucl. Phys. **10**, 422 (1970)].
[10]S.G. Kadmenskiĭ and V.E. Kalechits, Yad. Fiz. **12**, 70 (1971) [Sov. J. Nucl. Phys. **12**, 37 (1971)].
[11]S.G. Kadmenskiĭ, in: Materialy VII Zimneĭ Shkoly LIYaF po Fiziki Yadra i Elementarynykh Chastits [Proc. Seventh Winter School of the Leningrad Institute of Nuclear Physics on Nuclear Physics and Elementary Particles], Part II, Nauka, Leningrad (1972)
[12]S.G. Kadmenskiĭ, V.E. Kalechits, and A.A. Martynov, Yad. Fiz. **14**, 1174 (1972) [Sov. J. Nucl. Phys. **14**, 654 (1972).
[13]S.G. Kadmenskiĭ and V.G. Khlebostroev, Yad. Fiz. **18**, 980 (1974) [Sov. J. Nucl. Phys. **18**, 505 (1974)].
[14]J. Schwinger and B.A. Lippmann, Phys. Rev. **79**, 469 (1950).
[15]M.L. Goldberger and K.M. Watson, Collision Theory, New York (1964).
[16]H.-D. Zeh, Z. Phys. **175**, 490 (1963).
[17]A.B. Migdal, Theory of Finite Fermi Systems, Interscience, New York (1967).
[18]S.G. Kadmenskiĭ, Izv. Akad. Nauk SSSR, Ser. Fiz., **30**, 1349 (1966).
[19]A. Săndulescu, Rev. Roum. Phys. **15**, 1105 (1970).
[20]V.C. Aguilera-Navarro, M. Moshinsky, and W.W. Yeh, Ann. Phys. **51**, 312 (1969).
[21]T.A. Brody and M. Moshinsky, Tables of Transformation Brackets, Mexico (1960).
[22]V.I. Furman *et al.*, Nucl. Phys. A **226**, 131 (1974).
[23]S.G. Kadmenskiĭ *et al.*, Soobshchenie OIYaI [Preprint JINR] R4-8101 (1974).
[24]S.G. Kadmenskiĭ, V.E. Kalechits, and A.A. Martynov, Yad. Fiz., **13**, 300 (1971) [Sov. J. Nucl. Phys. **13**, 166 (1971)].
[25]S.G. Kadmenskiĭ, V.E. Kalechits, and A.A. Martynov, Yad. Fiz. **16**, 717 (1973) [Sov. J. Nucl. Phys. **16**, 400 (1973)].
[26]A.A. Martynov and S.G. Kadmenskiĭ, Yad. Fiz. **17**, 75 (1973) [Sov. J. Nucl. Phys. **17**, 39 (1973)].
[27]N.K. Glendenning and K. Harada, Nucl. Phys. **72**, 481 (1965).
[28]W.T. Pinkston, Nucl. Phys. **37**, 312 (1962).
[29]Y.E. Kim and J.O. Rasmussen, Nucl. Phys. **47**, 184 (1963).
[30]T.T. Kuo and G.H. Xerling, NRL-2258 (1971); M.B. Lewis and W.W. Daelinick, Phys. Rev. C **1**, 1577 (1970).
[31]V.G. Solov'ev, Vliyanie Parnykh Korrelyatsiĭ Sverkhprovodyashchego Tipa na Svoĭstva Atomnykh Yader [Influence of Pairing Correlations of Superconducting Type on the Properties of Nuclei], Gosatomizdat, Moscow (1963).
[32]V.G. Solov'ev, Dokl. Akad. Nauk SSSR **144**, 1281 (1962) [Sov. Phys.-Doklady **7**, 548 (1962)].
[33]K. Harada, Progr. Theor. Phys. **26**, 667 (1961).
[34]É.E. Sapershteĭn and M.A. Troitskiĭ, Yad. Fiz. **1**, 400 (1965) [Sov. J. Nucl. Phys. **1**, 284 (1965)].
[35]S.G. Kadmenskiĭ and K.S. Rybak, Yad. Fiz. **19**, 971 (1974) [Sov. J. Nucl. Phys. **19**, 499 (1974)].
[36]L.A. Sliv, G.A. Sogomova, and Yu.I. Kharitonov, Zh. Eksp. Teor. Fiz. **40**, 946 (1961) [Sov. Phys.-JETP **13**, 661 (1961)]; V.N. Guman, L.A. Sliv, and G.A. Sogomonova, Zh. Éksp. Teor. Fiz. **40**, 341 (1961) [Sov. Phys.-JETP **13**, 232 (1961)]; V.N. Guman *et al.*, Nucl. Phys. **28**, 192 (1961).
[37]V.G. Neudachin and Yu.F. Smirnov, Nuklonnye Assotsiatsii v Legkikh Yadrakh [Nucleon Clusters in Light Nuclei], Nauka, Moscow (1969).

[38]S. G. Kadmenskiĭ, A.A. Martynov, and Yu.I. Kharitonov, Yad. Fiz. 19, 529 (1974) [Sov. J. Nucl. Phys. 19, 267 (1974)].
[39]A. V. Boyarkina, Izv. Akad. Nauk. SSSR, Ser. Fiz., 28, 337 (1964).
[40]I.V. Kurdyumov *et al.*, Phys. Lett. B 40, 607 (1972).
[41]V.G. Neudatchin *et al.*, Nuovo Cimento Lett. 5, 834 (1972).
[42]R. Hofstadter, in: Electromagnetic Structure of Nuclei and Nucleons [Russian translation from the English], Izd-vo Inostr. Lit., Moscow (1958).
[43]V.M. Galitskiĭ, Zh. Éksp. Teor. Fiz. 34, 151 (1958) [Sov. Phys.-JETP 7, 104 (1958)].
[44]A.I. Baz', in: Materialy VII Zimneĭ Shkoly LIYaF po Fiziki Yadra i Élementarnykh Chastits [Proc. Seventh Winter School of the Leningrad Institute of Nuclear Physics on Nuclear Physics and Elementary Particles], Part I, Nauka, Leningrad (1972).
[45]L.K. Peker, in: Materialy IX Zimneĭ Shkoly LIYaF po Fiziki Yadra i Élementarynkh Chastits [Proc. Seventh Winter School of the Leningrad Institute of Nuclear Physics on Nuclear Physics and Elementary Particles], Part II, Nauka, Leningrad (1974).
[46]L. Scherk and E.W. Vogt, Canad. J. Phys. 46, 1119 (1968).
[47]A.A. Martynov, Yu.P. Popov, and V.I. Furman, in: Programma i Tezisy XX Soveshchaniya po Yadernoĭ Spektroskopii i Strukture Atomnogo Yadra [Program and Abstracts of 20th Conference on Nuclear Spectroscopy and Nuclear Structure], Part II, Nauka, Leningrad 251 (1970).
[48]Yu.P. Popov *et al.*, Yad. Fiz. 13, 913 (1971) [Sov. J. Nucl. Phys. 13, 523 (1971)].
[49]N. Cărjan and A. Săndulescu, Z. Naturf. B 26a, 1389 (1971).
[50]L. McFadden and G.R. Satchler, Nucl. Phys. 84, 177 (1966).
[51]Yu.P. Popov, in: Struktura Yadra [Structure of the Nucleus], Dubna (1972).
[52]Yu.P. Popov, in: Neĭtronnaya Fizika, Materialy Vsesoyuznogo Soveshchaniya, Kiev (1971) [Neutron Physics, Proc. All-Union Conference, Kiev, 1971], Naukova Dumka, Kiev 155 (1972).
[53]Yu.P. Popov *et al.*, in: Nuclear Data for Reactors, Vol. 1, IAEA, Vienna (1971).
[54]V.I. Furman and Yu.P. Popov, in: Neĭtronnaya Fizika, Materialy Vsesoyuznogo Soveshchaniya, Kiev (1971) [Neutron Physics, Proc. All-Union Conference, Kiev (1971)], Naukova Dumka, Kiev 159 (1972).
[55]W. Furman *et al.*, Phys. Lett. B 44, 465 (1973).
[56]V.G. Solov'ev, Fiz. Él. Chast. Atom. Yad. 3, 770 (1972) [Sov. J. Part. Nucl. 3, 390 (1973)].
[57]V.I. Furman and Yu.P. Popov, in: Programma i Tezisy XXIII Soveshchaniya po Yadernoĭ Spektroskopii i Strukture Atomnogo Yadra [Program and Abstracts of 20th Conference on Nuclear Spectroscopy and Nuclear Structure], Nauka, Leningrad (1973).
[58]V.I. Furman and Yu.P. Popov, Conference on Nuclear Structure Study with Neutrons, Budapest (1972).
[59]F.A. Gareev, S.P. Ivanova, and N.Yu. Shirikova, Preprint OIYaI R4-5457 [in Russian], JINR, Dubna (1970).
[60]S.A. Fayans, Preprint IAÉ-1593 [in Russian], I.V. Kurchatov Institute of Atomic Energy (1968).
[61]R. Bonetti and L. Milazzo-Colli, Phys. Lett. B 49, 17 (1974).
[62]S.G. Kadmenskiĭ, V.E. Kalechits, and G.A. Martynov, Yad. Fiz. 14, 343 (1971) [Sov. J. Nucl. Phys. 14, 193 (1972)].
[63]P. Hornshoj *et al.*, Nucl. Phys. (1974), (in press).
[64]G. Igo, Phys. Rev. 115, 1665 (1959).
[65]G. Breit, Theory of Resonance Nuclear Reactions [Russian translation from the English], Izd-vo Inostr. Lit., Moscow (1961).

Translated by Julian B. Barbour